Bulletin of the Seismological Society of America, Vol. 84, No. 4, pp. 974–1002, August 1994

New Empirical Relationships among Magnitude, Rupture Length, Rupture Width, Rupture Area, and Surface Displacement

by Donald L. Wells and Kevin J. Coppersmith

Abstract Source parameters for historical earthquakes worldwide are compiled to develop a series of empirical relationships among moment magnitude (**M**), surface rupture length, subsurface rupture length, downdip rupture width, rupture area, and maximum and average displacement per event. The resulting data base is a significant update of previous compilations and includes the additional source parameters of seismic moment, moment magnitude, subsurface rupture length, downdip rupture width, and average surface displacement. Each source parameter is classified as reliable or unreliable, based on our evaluation of the accuracy of individual values. Only the reliable source parameters are used in the final analyses. In comparing source parameters, we note the following trends: (1) Generally, the length of rupture at the surface is equal to 75% of the subsurface rupture length; however, the ratio of surface rupture length to subsurface rupture length increases with magnitude; (2) the average surface displacement per event is about one-half the maximum surface displacement per event; and (3) the average subsurface displacement on the fault plane is less than the maximum surface displacement but more than the average surface displacement. Thus, for most earthquakes in this data base, slip on the fault plane at seismogenic depths is manifested by similar displacements at the surface. Log-linear regressions between earthquake magnitude and surface rupture length, subsurface rupture length, and rupture area are especially well correlated, showing standard deviations of 0.25 to 0.35 magnitude units. Most relationships are not statistically different (at a 95% significance level) as a function of the style of faulting: thus, we consider the regressions for all slip types to be appropriate for most applications. Regressions between magnitude and displacement, magnitude and rupture width, and between displacement and rupture length are less well correlated and have larger standard deviation than regressions between magnitude and length or area. The large number of data points in most of these regressions and their statistical stability suggest that they are unlikely to change significantly in response to additional data. Separating the data according to extensional and compressional tectonic environments neither provides statistically different results nor improves the statistical significance of the regressions. Regressions for cases in which earthquake magnitude is either the independent or the dependent parameter can be used to estimate maximum earthquake magnitudes both for surface faults and for subsurface seismic sources such as blind faults, and to estimate the expected surface displacement along a fault for a given size earthquake.

Introduction

Seismic hazard analyses, both probabilistic and deterministic, require an assessment of the future earthquake potential in a region. Specifically, it is often necessary to estimate the size of the largest earthquakes that might be generated by a particular fault or earthquake source. It is rare, however, that the largest possible earthquakes along individual faults have occurred during the historical period. Thus, the future earthquake poten-

tial of a fault commonly is evaluated from estimates of fault rupture parameters that are, in turn, related to earthquake magnitude.

It has been known for some time that earthquake magnitude may be correlated with rupture parameters such as length and displacement (e.g., Tocher, 1958: Iida, 1959; Chinnery, 1969). Accordingly, paleoseismic and geologic studies of active faults focus on estimating these source characteristics. For example, data from geomorphic and geologic investigations of faults may be used to assess the timing of past earthquakes, the amount of displacement per event, and the segmentation of the fault zone (e.g., Schwartz and Coppersmith, 1986; Schwartz, 1988; Coppersmith, 1991). To translate these source characteristics into estimates of earthquake size, relationships between rupture parameters and the measure of earthquake size, typically magnitude, are required.

Numerous published empirical relationships relate magnitude to various fault rupture parameters. Typically, magnitude is related to surface rupture length as a function of slip type. Additional relationships that have been investigated include displacement versus rupture length, magnitude versus maximum surface displacement, magnitude versus total fault length, and magnitude versus surface displacement times surface rupture length (Tocher, 1958; Iida, 1959; Albee and Smith, 1966; Chinnery, 1969; Ohnaka, 1978; Slemmons, 1977, 1982; Acharya, 1979; Bonilla and Buchanon, 1970; Bonilla *et al.*, 1984; Slemmons *et al.*, 1989). Other studies relate magnitude and seismic moment to rupture length, rupture width, and rupture area as estimated from the extent of surface deformation, dimensions of the aftershock zone, or earthquake source time functions (Utsu and Seki, 1954; Utsu, 1969; Kanamori and Anderson, 1975; Wyss, 1979; Singh *et al.*, 1980; Purcaru and Berckhemer, 1982; Scholz, 1982; Wesnousky, 1986; and Darragh and Bolt, 1987).

The purpose of this article is to present new and revised empirical relationships between various rupture parameters, to describe the empirical data base used to develop these relationships, and to draw first-order conclusions regarding the trends in the relationships. Specifically, this article refines the data sets and extends previous studies by including data from recent earthquakes and from new investigations of older earthquakes. The new data provide a much larger and more comprehensive data base than was available for previous studies. Additional fault characteristics, such as subsurface rupture length, downdip rupture width, and average fault displacement, also are included. Because the new data set is more comprehensive than those used for previous studies, it is possible to examine relationships among various rupture parameters, as well as the relationships between rupture parameters and magnitude. An important goal of this article is to present the observational data base in a form that is sufficiently complete to enable the reader to reproduce our results, as well as to carry out subsequent analyses.

The following sections describe the observational data base, present the statistical relationships developed between magnitude and fault rupture parameters, and then evaluate the relationships in terms of their statistical significance, relative stability, and overall usefulness.

Data Base

A worldwide data base of source parameters for 421 historical earthquakes is compiled for this study. The data include shallow-focus (hypocentral depth less than 40 km), continental interplate or intraplate earthquakes of magnitudes greater than approximately 4.5. Earthquakes associated with subduction zones, both plate interface earthquakes and those occurring within oceanic slabs, are excluded. For each earthquake in the data base, we compiled seismologic source parameters and fault characteristics, including seismic moment, magnitude, focal mechanism, focal depth, slip type, surface and subsurface rupture length, maximum and average surface displacement, downdip rupture width, and rupture area.

In general, the data presented in this article are obtained from published results of field investigations of surface faulting and seismologic investigations. For many earthquakes, there are several published measurements of various parameters. One objective of this study is to identify the most accurate value for each parameter, or the average value where the accuracy of individual values could not be determined. Special emphasis is placed on identifying the sources and types of measurements reported in the literature (e.g., rupture area based on aftershock distribution, geodetic modeling, or teleseismic inversion). All data are then categorized by type of measurement, and the most accurate value is selected for further analysis. The data selection process for each rupture parameter is described in detail in the following sections.

From the larger data base, 244 earthquakes are selected to develop empirical relationships among various source parameters. For these earthquakes, which are listed in Table 1, the source parameters are considered much more reliable than the source parameters for the other earthquakes. Earthquakes that are evaluated but excluded from further study because of insufficient information or poor-quality data are provided on microfiche (Appendix A). Each earthquake listed in Table 1 is identified by location, name (geographic descriptor or associated fault), and date of origin in Coordinated Universal Time (UTC). Each source parameter given in Table 1 is discussed below.

Slip Type

Past studies have demonstrated that the slip type or style of faulting is potentially significant for correlating earthquake magnitude and rupture parameters (e.g.,

Table 1
Earthquake Source Parameters*

EQN	Location	Earthquake	Date (UTC, m/d/yr)	Slip Type**	M_S†	M††	Seismic Moment‡ (10^{26} dyne-cm)		Rupture Length (km)†† Surface	Rupture Length (km)†† Subsurface	Rupture Width†† (km)	Rupture Area†† (km^2)	Displacement (m)†† Maximum	Displacement (m)†† Average
1	USA, CA	Fort Tejon	01/09/1857	RL	8.3 [I]	(7.85)	670	[1]	297		12‡‡	(4296)	9.4	6.4#
2	USA, CA	Hayward	10/21/1868	RL	6.8 [I]	(6.76)	15.6	[1]	48		12‡‡	(576)	0.9	
3	USA, CA	Owens Valley	03/26/1872	RL-N	8.0 [I]	(7.61)	292	[1]	108		15‡‡	(1620)	11.0	6.0
4	Mexico	Pitaycachi	05/03/1887	N	7.4 [I]	(7.31)	105	[1]	75				4.5	1.9
5	Japan	Nobi	10/27/1891	LL	8.0 [I]	(7.49)	190	[1]	80		15‡‡	(1200)	8.0	5.04#
6	Japan	Rikuu/Senya	08/31/1896	R	7.2 [J]	(7.40)	140	[1]	40		(21)‡‡	(840)	4.4	2.59#
7	USA, CA	San Francisco	04/18/1906	RL	7.8 [B]	7.90	790	[5]	432		12‡‡	5184	6.1	3.3#
8	Italy	Avezzano	01/13/1915	N	7.0 [G]	(6.62)	9.7	[2]	20	24¶	15¶	360¶	2.0	
9	USA, Nevada	Pleasant Valley	10/03/1915	N	7.6 [L]	(7.18)	66	[1]	62		15‡‡	(930)	5.8	2.0
10	China	Kansu	12/16/1920	LL	8.5 [G]	8.02	1200	[3]	220		(20)‡‡	(4400)	10.0	7.25#
11	Japan	Tango	03/07/1927	LL-R	7.7 [L]	(7.08)	46	[1]	(14)	(35)	15	525	(3.0)	
12	Kenya	Laikipia	01/06/1928	N	7.0 [L]				31				3.3	
13	Bulgaria	Papazili	04/18/1928	N	6.9 [L]	(7.13)	55	[1]	50				3.5	
14	Iran	Salmas	05/06/1930	N-RL	7.4 [L]	(7.15)	60	[1]	30				6.4	1.35
15	Japan	North Izu	11/25/1930	LL-R	7.3 [L]	6.89	24	[5]	35	(22)¶	(12)‡‡	(420)	3.8	2.9
16	New Zealand	Hawkes Bay	02/02/1931	R-RL	7.8 [G]	(7.73)	440	[2]	15	(110)			(4.6)	
17	China	Kehetuohai-E	08/10/1931	RL	7.9 [L]	7.92	850	[3]	180		(20)‡‡	(3600)	14.6	7.38#
18	Japan	Saitama	09/21/1931	LL	6.7 [G]	(6.52)	6.8	[1]		20	10	200		
19	USA, Nevada	Cedar Mountain	12/21/1932	RL	7.2 [G]	6.83	19.7	[3]	61	(80)			2.0	
20	China	Changma	12/25/1932	R-LL	7.7 [L]	(7.60)	280	[1]	148				4.0	2.0
21	USA, CA	Long Beach	03/11/1933	RL	6.3 [G]	6.38	4.1	[5]		23	13	300		
22	Japan	South Izu	03/21/1934	RL	5.5 [J]	(5.29)	0.095	[1]		7§	4	28§		
23	Taiwan	Tuntzuchio/Chih.	04/21/1935	RL-R	7.1 [G]				(17)				2.1	
24	Turkey	Kirsehir	04/19/1938	RL	6.8 [L]				14				1.0	
25	Turkey	Erzihcan	12/26/1939	RL	7.8 [L]	(7.81)	575	[1]	360		(20)‡‡	(7200)	7.5	(1.85)
26	USA, CA	Imperial Valley	05/19/1940	RL	7.2 [L]	6.92	27	[5]	60	(45)§	11‡‡	(660)	5.9	1.5
27	Turkey	Erbaa	12/20/1942	RL-N	7.2 [L]	(6.90)	25	[1]	47		(10)‡‡	(500)	2.0	0.66
28	Japan	Sikano	09/10/1943	RL	7.4 [L]	(7.00)	36	[1]	(4.7)	33	13	429	(1.5)	(0.5)
29	Turkey	Kastamonu	11/26/1943	RL	7.5 [L]	(7.58)	260	[1]	280		(14)‡‡	(3920)	(1.9)	(0.57)
30	Turkey	Bolu	02/01/1944	RL	7.5 [L]	(7.59)	270	[1]	180		(20)‡‡	(3600)	3.6	1.8
31	Turkey	Ustukran	05/31/1946	RL	6.0 [G]				9				0.3	
32	Peru	Ancash	11/10/1946	N	7.2 [G]	7.28	94	[3]	21	28§	30§	840§	3.5	
33	Taiwan	Tainan	12/04/1946	RL	6.7 [L]				12				2.1	
34	Japan	Fukui	06/28/1948	LL-R	7.3 [G]	(6.98)	33	[1]		30	13	390		
35	USA, CA	Desert Hot Spring	12/04/1948	RL	6.5 [G]	(5.97)	1	[3]		15	(16)			
36	Turkey	Elmalidere	08/17/1949	RL	6.9 [A]				38				1.6	0.9
37	Japan	Imaichi	12/26/1949	R?	6.3 [G]					11	7	77		
38	USA, CA	Fort Sage Mtns.	12/14/1950	N	5.6 [G]				9.2				0.20	
39	USA, CA	Superstition Hills	01/23/1951	RL	5.6 [M_L]				3				(0.05)	
40	China	Damxung	11/18/1951	RL	8.0 [G]	7.67	365	[5]	90	200	(10)‡‡	(2000)	12.0	8.0
41	Taiwan	Yuli-Juisu	11/24/1951	LL-R	7.4 [L]	(7.08)	46	[1]	43		(17)‡‡	(731)	2.1	
42	USA, CA	Kern County	07/21/1952	R-LL	7.7 [L]	7.38	130	[5]	57	64	19	1216	3.0	0.6
43	Turkey	Canakkale	03/18/1953	RL	7.2 [L]	7.22	77	[3]	58		(18)‡‡	(1080)	4.35	2.1#
44	USA, CA	Arroyo Salada	03/19/1954	RL	6.2 [D]	6.27	2.89	[5]		15	12	180		

Table 1—*Continued*

EQN	Location	Earthquake	Date (UTC, m/d/yr)	Slip Type**	M_S†	M††	Seismic Moment‡ (10^{26} dyne-cm)	Rupture Length (km)†† Surface	Rupture Length (km)†† Subsurface	Rupture Width†† (km)	Rupture Area†† (km^2)	Displacement (m)†† Maximum	Displacement (m)†† Average
45	USA, Nevada	Rainbow Mountain	07/06/1954	N	6.3 [L]	6.22	2.4 [5]	18	(11)§	14‡‡	(252)	0.31	0.25
46	USA, Nevada	Stillwater	08/24/1954	N	6.9 [L]	6.55	7.6 [5]	34	(26)§	14‡‡	(428)	0.76	0.45
47	USA, Nevada	Fairview Peak	12/16/1954	RL-N	7.2 [L]	7.17	64 [5]	57	(50)¶	15	(855)	4.1	2.8
48	USA, Nevada	Dixie Valley	12/16/1954	RL-N	6.8 [PS]	6.94	29 [5]	45	(42)¶	14‡‡	(630)	3.8	2.1
49	Mexico	San Miguel	02/09/1956	RL-R	6.9 [L]	6.63	10 [5]	22	(22)§	12‡‡	(264)	0.9	0.5
50	USA, CA	San Francisco	03/22/1957	N	5.3 [M_L]	5.21	0.074 [3]		7	5	35		
51	Turkey	Abant	05/26/1957	RL	7.0 [A]			40		(8)‡‡	(320)	1.65	0.55
52	Mongolia	Gobi-Altai	12/04/1957	LL	7.9 [L]	8.14	1800 [3]	236	300	(20)‡‡	(6000)	9.4	6.54#
53	USA, Alaska	Lituya Bay	07/10/1958	RL	7.9 [U]	7.77	510 [5]	(200)	350	12	4200	(6.6)	
54	USA, MT	Hebgen Lake	08/18/1959	N	7.6 [L]	7.29	95 [3]	26.5	45	17	765	6.1	2.14
55	USA, Utah	Cache Valley	08/30/1962	N	5.7 [M_L]	5.78	0.52 [5]		7	8	56		
56	Iran	Ipak	09/01/1962	R	7.2 [L]	(7.35)	117 [1]	99				0.8	
57	Japan	Wakasa-Bay	03/26/1963	RL	6.5 [D]	6.28	3 [5]		20	8	160		
58	Yugoslavia	Skopje	07/26/1963	LL-N	6.1 [A]	5.99	1.1 [3]	(6)	17	11	187	(0.1)	
59	USA, CA	Watsonville	09/14/1963	RL	5.4 [U]	5.17	0.063 [3]		7	3.5	25		
60	Japan	Niigata	06/16/1964	R	7.5 [B]	7.59	273 [5]	(40)	60	30	1800		
61	USA, CA	Corralitos	11/16/1964	RL	5.1 [M_L]				4	4	16		
62	USA, CA	Antioch	09/10/1965	RL	4.9 [M_L]				3	6	18		
63	USA, CA	Parkfield	06/28/1966	RL	6.4 [W]	6.25	2.7 [5]	38.5	35	10	350	0.20	
64	USA, Nevada	Caliente-Clover Mtn.	08/16/1966	RL	5.8 [M_L]	5.58	0.26 [5]		11	6	66		
65	Turkey	Varto	08/19/1966	RL	6.8 [B]	6.88	23.5 [3]	30	(85)	(10)‡‡	(300)	0.4	0.15
66	USA, CA	Truckee	09/12/1966	LL	5.9 [PB]	5.96	0.97 [5]		13	7	91		
67	Mongolia	Mogod	01/05/1967	RL	7.4[L]	7.03	39 [5]	40	40	(20)‡‡	(800)	1.3	
68	Turkey	Mudurna Valley	07/22/1967	RL	7.4 [L]	7.34	113 [5]	80	(70)	(20)‡‡	(1600)	2.6	1.63#
69	Albania	Dibra	11/30/1967	RL-N	6.6 [A]	6.75	15 [3]	10	(62)			0.5	0.2
70	Greece	Agios-Efstratios	02/19/1968	RL	7.2 [B]	7.10	50.8 [5]	(4.4)	70			(0.5)	
71	USA, CA	Borrego Mountain	04/09/1968	RL	6.8 [L]	6.63	10 [5]	31	40	10	400	0.38	0.18#
72	New Zealand	Glasgow	05/24/1968	R-LL	7.1 [U]	(7.07)	45 [2]	(2)	41	18	738	(0.52)	
73	Iran	Dasht-e-Bayaz	08/31/1968	LL	7.1 [L]	7.23	78 [5]	80	110	20	2200	5.2	2.3
74	Australia	Meckering	10/14/1968	R-RL	6.9 [L]	6.61	9.3 [5]	36	20¶	10	200¶	3.5	0.9#
75	USA, Alaska	Rampart	10/29/1968	LL	6.5 [U]	6.69	12 [3]		30	8	240		
76	Turkey	Alasehir Valley	03/28/1969	N	6.5 [A]	6.71	13 [5]	32	30	(11)‡‡	(330)	0.82	0.54
77	USA, CA	Coyote Mountain	04/28/1969	RL-N	5.8 [M_L]	5.69	0.38 [5]		10	3	30		
78	Peru	Pariahuanca	07/24/1969	R	5.7 [U]	6.14	1.81 [3]	(5.5)				0.4	
79	China	Yangjiang	07/25/1969	RL-N	5.9 [U]	5.77	0.515 [3]		11				
80	Japan	Gifu	09/09/1969	RL	6.6 [J]	6.34	3.6 [5]		18	10	180	(0.72)	
81	South Africa	Ceres	09/29/1969	RL	6.3 [U]	6.37	4 [5]		20	9	180		
82	Peru	Huaytapallana	10/01/1969	R-LL	6.2 [U]	6.63	9.84 [3]	(16)	30			1.2	
83	China	Tonghai	01/04/1970	RL	7.5 [L]	7.26	87 [5]	48	75	(15)‡‡	(1125)	2.7	2.1
84	Turkey	Gediz	03/28/1970	N	7.1 [L]	7.18	67 [5]	41	63	(17)‡‡	(1071)	2.8	0.86#
85	Japan	Akita	10/16/1970	R-RL	5.8 [U]	6.13	1.75 [5]		14	11	154		
86	USA, CA	San Fernando	02/09/1971	R-LL	6.5 [L]	6.64	10.4 [5]	16	17	14	238	2.5	1.5#
87	Turkey	Bingol	05/22/1971	LL	6.7 [U]	6.63	10 [3]	38				0.6	(0.25)
88	USA, CA	Bear Valley	02/24/1972	RL	5.1 [M_L]	5.23	0.078 [3]		6	3	18		
89	USA, CA	Bear Valley	02/27/1972	LL	4.7 [M_L]	4.57	0.008 [3]		3.8	2.5	9.5		

Table 1—*Continued*

EQN	Location	Earthquake	Date (UTC, m/d/yr)	Slip Type**	M_S†	M††	Seismic Moment‡ (10^{26} dyne-cm)		Rupture Length (km)†† Surface	Rupture Length (km)†† Subsurface	Rupture Width†† (km)	Rupture Area†† (km^2)	Displacement (m)†† Maximum	Displacement (m)†† Average
90	Iran	Qir-Karzin	04/10/1972	R	6.9 [A]	6.75	15	[3]	(20)	34	(20)‡‡	(680)‡‡	(0.1)	
91	USA, Alaska	Sitka	07/30/1972	RL	7.6 [U]	7.70	400	[5]		180	10	1800		
92	Pakistan	Hamran	09/03/1972	R	6.3 [m_b]	6.19	2.2	[3]		13	(14)‡‡	(168)§		
93	USA, CA	Stone Canyon	09/04/1972	RL	4.7 [M_L]	4.83	0.02	[3]		2.6	2.3	6		
94	USA, CA	San Juan Bautista	10/03/1972	RL	4.8 [M_L]	4.77	0.016	[3]		4.3	2.5	11		
95	Nicaragua	Managua	12/23/1972	LL	6.2 [L]	(6.31)	3.3	[1]	(5.9)	15	8	120	(0.67)	
96	China	Luhuo	02/06/1973	LL	7.3 [L]	7.47	180	[5]	89	110	13	1430	3.6	1.3
97	USA, CA	Point Mugu	02/21/1973	R	5.2 [U]	5.72	0.42	[5]		8	3.3§	25		
98	China	Tibet	07/14/1973	N	6.9 [U]	6.95	29.6	[5]		(27)§		600		
99	USA, CA	Agua Caliente Spr.	09/13/1973	RL	4.8 [M_L]					3				
100	Japan	Izu-Oki	05/08/1974	RL-R	6.5 [U]	6.54	7.2	[5]	(5.7)	18	11	198	(0.48)	
101	Japan	Amagi	07/09/1974	LL-N	4.9 [J]	(4.97)	0.032	[1]		3.5	3	10.5	(0.09)	
102	USSR	Tadzhikestan	08/11/1974	R-RL	7.3 [U]	7.06	43.8	[5]		30	20	600		
103	USA, CA	Brawley	01/23/1975	RL	4.6 [U]				(10.4)	9	4	36	(0.20)	
104	China	Haicheng	02/04/1975	LL	7.4 [U]	6.99	34.5	[5]	(5.5)	60	15	900	(0.55)	
105	USA, Idaho	Pocatello Valley	03/28/1975	N	6.0 [U]	6.06	1.4	[5]		15	10	150		
106	Japan	Oita Prefecture	04/20/1975	LL-R	6.1 [U]	6.32	3.4	[3]		10	10	100		
107	USA, CA	Galway Lake	05/31/1975	RL	5.2 [U]				6.8	5	3	15	0.02	
108	USA, WY	Yellowstone	06/30/1975	N-RL	5.9 [U]	5.88	0.75	[3]		10	5	50		
109	USA, CA	Oroville	08/01/1975	N-RL	5.6 [U]	6.01	1.18	[5]	3.8	8	10	80	0.06	
110	USA, CA	Horse Canyon	08/02/1975	RL	4.7 [M_L]	5.00	0.035	[5]		2	2	4		
111	Turkey	Lice	09/06/1975	R	6.7 [U]	6.55	7.4	[5]	26		(13)‡‡	(234)	0.63	0.5
112	Guatemala	Motagua	02/04/1976	LL	7.5 [L]	7.63	310	[5]	235	257	13	3341	3.4	2.6#
113	USSR	Uzbekistan	04/08/1976	R	7.0 [U]	6.83	19.5	[5]		30	20	600		
114	Italy	Friuli	05/06/1976	R	6.5 [U]	6.49	6	[5]		19	10	190		
115	USSR	Uzbekistan	05/17/1976	R	7.0 [U]	6.84	20.7	[5]		48	24	1152		
116	China	Tangshan	07/27/1976	RL	7.9 [U]	7.46	176	[5]	(10)	70	24	1680	(3.0)	
117	China	Songpan, Huya	08/16/1976	LL-R	6.9 [U]	6.71	13	[3]		30	12	360		
118	Japan	Kawazu	08/17/1976	RL	5.4 [J]	(5.51)	0.21	[1]		9	4	32		
119	China	Songpan, Huya	08/21/1976	R	6.4 [U]	6.37	4	[3]		12	8	96		
120	China	Songpan, Huya	08/23/1976	LL-R	6.7 [U]	6.58	8.4	[3]		22	11	242		
121	Turkey	Caldiran	11/24/1976	RL	7.3 [L]	7.23	79	[5]	55	(90)§	(18)‡‡	(1620)§	3.5	2.05
122	Mexico	Mesa de Andrade	12/07/1976	RL	5.7 [U]	5.61	0.29	[3]		9	5	45		
123	Iran	Khurgu	03/21/1977	R	6.9 [U]	6.73	14	[4]		32				
124	New Zealand	Matata	05/31/1977	RL-N	5.4 [M_L]	5.61	0.29	[3]		8.5	5	42		
125	USA, Utah	Unita Basin	09/30/1977	N	5.1 [M_L]					2	3	6		
126	USA, CA	Willits	11/22/1977	RL	4.8 [M_L]	5.24	0.082	[4]		5	7.5	20		
127	Argentina	Caucete	11/23/1977	R	7.4 [U]	7.48	189	[5]		80	30	2400		
128	Iran	Bob-Tangol	12/19/1977	RL	5.8 [L]	5.89	0.76	[4]	12	14	12	168	0.30	0.12
129	Japan	Izu-Oshima	01/14/1978	RL	6.6 [U]	6.71	13.2	[5]	(3.2)	50	10	500	(1.0)	
130	USA, WA	South Puget Sound	03/11/1978	RL	4.8 [M_L]					2.5	4	10		
131	Greece	Thessaloniki	06/20/1978	N	6.4 [U]	6.43	5.02	[5]	19.4	28	14	392	0.22	0.08#
132	USA, CA	Santa Barbara	08/13/1978	R-LL	5.6 [U]	5.88	0.75	[5]		10	5	50		
133	Germany	Swabian Jura	03/09/1978	LL	5.3 [U]	5.21	0.074	[5]		4.5	6	27		
134	USA, CA	Diamond Valley	09/04/1978	RL	5.2 [M_L]					1.7				

Table 1—*Continued*

EQN	Location	Earthquake	Date (UTC, m/d/yr)	Slip Type**	M_S†	M††	Seismic Moment‡ (10^{26} dyne-cm)	Rupture Length (km)††		Rupture Width†† (km)	Rupture Area†† (km^2)	Displacement (m)††	
								Surface	Subsurface			Maximum	Average
135	Iran	Tabas-e-Golshan	09/16/1978	R	7.5 [L]	7.39	137 [5]	85	74	22	1628	3.0	1.5
136	USA, CA	Wheeler Crest	10/04/1978	N	5.1 [U]	5.47	0.18 [4]		7	5.5	38		
137	USA, CA	Malibu	01/01/1979	R	4.7 [U]				5	5	25		
138	USA, CA	Homestead Valley	03/15/1979	RL	5.6 [U]	5.55	0.241 [4]	3.9	6	4	24	0.10	0.05
139	Yugoslavia	Montenegro	04/15/1979	R	6.9 [U]	6.98	32.9 [5]		50	29	1450		
140	Australia	Cadoux	06/02/1979	R	6.1 [U]	6.12	1.67 [5]	15	16	6	96	1.5	0.5
141	USA, CA	Coyote Lake	08/06/1979	RL	5.7 [U]	5.77	0.51 [5]	14.4	14	10	140	0.15	
142	Canada	Charlevoix, Quebec	08/19/1979	R-RL	4.5 [U]	4.75	0.015 [5]		2	2	4		
143	Italy	Umbria, Norca	09/19/1979	RL-N	5.9 [U]	5.83	0.63 [5]		10	11	110		
144	USA, CA	El Centro	10/15/1979	RL	6.7 [L]	6.53	7.12 [5]	30.5	51	12	612	0.80	0.18#
145	Iran	Kurizan	11/14/1979	RL-R	6.7 [L]	6.61	9.1 [5]	17	28	(6)‡‡	(168)	1.1	
146	Iran	Koli	11/27/1979	LL-R	7.1 [L]	7.17	63 [5]	65	75	(22)‡‡	(1650)	3.9	1.2
147	England	Carlisle	12/26/1979	N-RL	4.8 [M_L]				4	3	12		
148	USA, CA	Greenville	01/24/1980	RL	5.9 [U]	5.82	0.6 [5]	6.2	11.5	12	138	0.03	
149	USA, CA	Anza	02/25/1980	RL	4.7 [U]	5.04	0.041 [5]		2.5	2.5	6		
150	France	Arudy	02/29/1980	N	4.9 [m_b]	5.17	0.064 [4]		3.8	5	19		
151	USA, CA	Mammoth Lakes	05/27/1980	LL	6.1 [U]	5.99	1.09 [5]		9	11	99		
152	Mexico	Mexicali Valley	06/09/1980	RL	6.4 [U]	6.40	4.5 [5]		28	8	224		
153	Japan	Izu-Hanto-Toho	06/29/1980	LL	6.2 [U]	6.39	4.3 [5]		14	10	140		
154	Greece	Almyros	07/09/1980	N	6.4 [U]	6.59	8.71 [4]	(5.3)	36			0.2	
155	USA, KY	Sharpsburg	07/27/1980	RL	4.7 [U]	5.06	0.043 [5]		4	5	20		
156	Algeria	El Asnam	10/10/1980	R	7.3 [L]	7.10	50.8 [5]	31.2	55	15	825	6.5	1.54#
157	Italy	South Apennines	11/23/1980	N	6.9 [U]	6.91	26 [5]	38	60	15	900	1.15	0.64
158	China	Daofu	01/23/1981	LL	6.8 [U]	6.64	10.1 [5]	44	46	15	690	1.5	
159	USA, WA	Elk Lake	02/14/1981	RL	4.8 [U]	5.30	0.1 [4]		6	7	42		
160	Greece	Corinth	02/24/1981	N	6.7 [U]	6.63	10 [5]	(15)	30	16	480		
161	Greece	Corinth	02/25/1981	N	6.4 [U]	6.31	3.28 [5]	19		16	400§	1.5	0.6
162	Greece	Corinth	03/04/1981	N	6.4 [U]	6.25	2.65 [5]	(13)	26	18	468	1.1	0.6
163	Iran	Golbaf	06/11/1981	R-RL	6.7 [U]	6.57	8.07 [5]	15	16		(580)	0.11	0.06
164	Iran	Sirch	07/28/1981	R-RL	7.1 [U]	7.12	53.5 [5]	65	75		(1002)	0.50	0.16
165	Canada	Miramichi	01/09/1982	R	5.2 [U]	5.55	0.24 [5]		5.5	4	22		
166	USA, CA	Anza	06/15/1982	RL	4.8 [M_L]	4.79	0.017 [5]		2.5	3	7.5		
167	USA, CA	New Idria	10/25/1982	R-LL	5.2 [U]	5.46	0.172 [5]		9				
168	North Yemen	Dhamer	12/13/1982	N	6.0 [U]	6.34	3.64 [5]	15	20	7	140	(0.03)	
169	Columbia	Popayan	03/31/1983	SS/N	4.9 [U]	5.66	0.35 [4]	1.3				(0.01)	
170	USA, CA	Coalinga	05/02/1983	R-LL	6.5 [U]	6.38	4.1 [5]		27	15	405		
171	Taiwan	Taipingshan	05/10/1983	N	5.4 [U]	5.72	0.427 [4]		9	(20)	(180)		
172	USA, CA	Coalinga, Nunez	06/11/1983	R	5.4 [U]	5.42	0.15 [5]	3.3	8	6.5	52	0.64	
173	USA, NY	Goodnow	10/07/1983	R	5.1 [M_L]	4.89	0.024 [5]		1.5	2	4		
174	USA, Idaho	Borah Peak	10/28/1983	N-LL	7.3 [U]	6.93	28 [5]	34	33	20	660	2.70	0.8
175	Turkey	Pasinier	10/30/1983	LL-R	6.9 [U]	6.73	14 [5]	12	50	16	800	1.2	
176	Belgium	Liege	11/08/1983	RL-R	4.3 [A]	4.77	0.016 [3]		5	3	15		
177	West Africa	Guinea	12/22/1983	RL-N	6.2 [U]	6.32	3.40 [5]	9.4	27	14	378	0.45	
178	USA, CA	Morgan Hill	04/24/1984	RL	6.1 [U]	6.28	3.0 [5]		26	8	208		
179	Italy	Perugia	04/29/1984	N	5.3 [U]	5.65	0.35 [5]		17	5	85		

Table 1—*Continued*

EQN	Location	Earthquake	Date (UTC, m/d/yr)	Slip Type**	M_S†	M††	Seismic Moment‡ (10^{26} dyne-cm)	Rupture Length (km)†† Surface	Rupture Length (km)†† Subsurface	Rupture Width†† (km)	Rupture Area†† (km^2)	Displacement (m)†† Maximum	Displacement (m)†† Average
180	Italy	Lazio-Abruzzo	05/07/1984	N	5.8 [U]	6.00	1.12 [5]		4.5	10	40		
181	Great Britan	North Wales	07/10/1984	SS-N	4.7 [U]	(4.63)	0.01 [3]		3	3.2	9.6		
182	USA, Alaska	Sutton, Talkeetn	08/14/1984	RL	5.2 [U]	5.84	0.64 [4]		8	6	48		
183	Japan	Naganoken-Seibu	09/14/1984	RL	6.1 [U]	6.24	2.6 [4]		12	8	104		
184	USA, WY	Laramie	10/18/1984	RL-N	5.1 [U]	5.31	0.102 [5]		3	3	9		
185	USA, CA	Round Valley	11/23/1984	LL	5.7 [U]	5.83	0.62 [5]		7	7	49		
186	Argentina	Mendoza	01/26/1985	R	5.9 [U]	5.87	0.72 [5]		16	16	256		
187	New Guinea	New Britan	05/10/1985	LL	7.1 [U]	7.19	69.3 [4]		50	15	750		
188	New Guinea	New Ireland	07/03/1985	R	7.2 [U]	7.23	79 [5]		48	23	1104		
189	USA, CA	Kettleman Hills	08/04/1985	R	5.9 [U]	6.09	1.53 [5]		20	8.3	166		
190	China	Wuqai	08/23/1985	R	7.3 [U]	6.89	24.6 [5]	15	(12)§			1.55	
191	Canada	Nahanni	10/05/1985	R	6.6 [U]	6.64	10.2 [5]		32	16	512		
192	Algeria	Constantine	10/27/1985	LL	5.9 [U]	6.00	1.11 [5]	3.8	21	13	273	0.12	0.10
193	Canada	Nahanni	12/23/1985	R	6.9 [U]	6.75	15 [5]		40	17	680		
194	USA, CA	Tres Pinos	01/26/1986	RL	5.3 [U]	5.42	0.15 [3]		11	5	55		
195	USA, Ohio	Painesville	01/31/1986	RL	5.0 [m_b]	4.87	0.023 [5]		1.5	2	3		
196	Canada	Prince George, BC	03/21/1986	R-RL	5.2 [U]	5.54	0.23 [5]		6	8	48		
197	Australia	Marryat Creek	03/30/1986	R-LL	5.8 [U]	5.79	0.54 [5]	13	13§	3§	39§	1.3	0.5
198	USA, CA	Mt Lewis	03/31/1986	RL	5.5 [U]	5.64	0.32 [5]		5.5	4	22		
199	Peru	Cuzco	04/05/1986	N	4.6 [U]	5.22	0.077 [4]	2.5				0.1	
200	Taiwan	Hualien	05/20/1986	R	6.4 [U]	6.37	4 [5]		20	24	480		
201	USA, CA	No. Palm Springs	07/08/1986	RL-R	6.0 [U]	6.13	1.73 [5]	(9)	16	9	144		
202	USA, CA	Oceanside	07/13/1986	R	5.8 [U]	5.87	0.73 [5]		8	7	56		
203	USA, CA	Chalfant Valley	07/21/1986	RL	6.2 [U]	6.31	3.2 [5]	(15.8)	20	11	220	(0.11)	
204	Greece	Kalamata	09/13/1986	N	5.8 [U]	5.93	0.89 [5]	15	15	14	210	0.18	0.15
205	El Salvador	San Salvador	10/10/1986	LL	5.4 [U]	5.74	0.45 [4]		6	7.5	45		
206	Taiwan	Hualien	11/14/1986	R	7.8 [U]	7.33	110 [5]		48	26	1248		
207	Japan	Omachi	12/30/1986	LL-R	5.3 [U]	5.51	0.21 [5]		7	4	28		
208	Mexico	Cerro Prieto	02/07/1987	LL	5.5 [U]	5.63	0.31 [5]		5				
209	New Zealand	Edgecumbe	03/02/1987	N	6.6 [U]	6.50	6.3 [5]	18	32	14	448	2.90	1.7
210	Japan	Kameoka	05/28/1987	N	4.9 [M_L]				1.4	1.8	2.5		
211	USA, Illinois	Wabash Valley	06/10/1987	RL	4.4 [U]	4.96	0.031 [3]		1.7	3	5		
212	China	Xunwu	08/02/1987	LL-N	4.8 [I]	5.01	0.036 [3]		4	4	16		
213	USA, Utah	Lakeside	09/25/1987	RL	4.6 [U]	5.02	0.038 [3]		5.5	6	30		
214	USA, CA	Whittier Narrows	10/01/1987	R	5.7 [U]	6.01	1.04 [5]		5	6	30		
215	USA, CA	Elmore Ranch	11/24/1987	LL	6.2 [U]	6.20	2.6 [5]	10	30	12	360	0.20	(0.23)
216	USA, CA	Superstition Hills	11/24/1987	RL	6.6 [U]	6.61	9.2 [5]	27	30	11	330	0.92	0.54
217	Australia	Tennant Creek	01/22/1988	R	6.3 [U]	6.26	2.8 [5]	10.2	13	9	117	1.3	0.63
218	Australia	Tennant Creek	01/22/1988	R-LL	6.4 [U]	6.38	4.1 [5]	6.7	13	9	117	1.17	0.60
219	Australia	Tennant Creek	01/22/1988	R	6.7 [U]	6.58	8.2 [5]	16	19	12	228	1.9	0.93
220	USA, Utah	Colorado Plateau	08/14/1088	LL-N	5.3 [M_L]				5	7	35		
221	China	Lancang-Gengma	11/06/1988	RL	7.3 [U]	7.13	54.7 [5]	35	80	20	1600	1.5	0.7
222	China	Gengma, Yunnan	11/06/1988	RL	7.2 [C]	6.83	20 [3]	15.6	46			1.1	0.6
223	Canada	Saguenay	11/25/1988	R	5.8 [U]	5.84	0.64 [5]		23	10	230		
224	USA, CA	Pasadena	12/03/1988	LL	4.2 [U]	4.96	0.031 [3]		4.5	2.5	10		

Table 1—*Continued*

EQN	Location	Earthquake	Date (UTC, m/d/yr)	Slip Type**	M_S†	M††	Seismic Moment‡ (10^{26} dyne-cm)	Rupture Length (km)†† Surface	Rupture Length (km)†† Subsurface	Rupture Width†† (km)	Rupture Area†† (km^2)	Displacement (m)†† Maximum	Displacement (m)†† Average
225	USSR	Armenia	12/07/1988	R-RL	6.8 [U]	6.76	15.3 [5]	25	38	11	418	2.0	
226	USA, Utah	South Wasatch	01/30/1989	LL	4.8 [U]	5.33	0.11 [4]		5	4	20		
227	USA, CA	Loma Prieta	10/18/1989	RL-R	7.1 [U]	6.92	267 [5]		40	16	640		
228	Algeria	Chenoua	10/29/1989	R	5.7 [U]	5.98	1.04 [4]	4.0	15	10	150	0.13	
229	Canada	Ungava	12/25/1989	R	6.3 [U]	5.98	1.04 [4]	10	10	5	50	2.0	0.8
230	Japan	Izu-Oshima	02/20/1990	LL	6.4 [U]	6.37	4.05 [5]		19	12	228		
231	USA, CA	Upland	02/28/1990	LL	5.5 [U]	5.59	0.27 [5]		4	7	28		
232	Iran	Rudbar-Tarom	06/20/1990	R-LL	7.7 [U]	7.41	147 [5]	80	(90)			0.95	
233	Philippines	Luzon	07/16/1990	LL	7.8 [U]	7.74	460 [5]	120	120	20	2400	6.2	
234	USA, CA	Lee Vining	10/24/1990	RL	5.2 [U]	5.33	0.11 [4]		4	4	16		
235	Japan	Southern Niigata	12/07/1990	R	5.1 [U]	5.28	0.092 [4]		6.5	5	33		
236	USA, CA	Sierra Madre	06/28/1991	R-LL	5.1 [U]	5.62	0.30 [5]		4	5	20		
237	USA, CA	Ragged Point	09/17/1991	R-RL	4.5 [U]	5.10	0.05 [4]		1.1	2	2.2		
238	Turkey	Erzincan	03/13/1992	RL	6.8 [U]	6.87	22.8 [5]	(30)	38			(0.20)	
239	USA, CA	Joshua Tree	04/23/1992	RL	6.3 [U]	6.27	2.9 [5]		15	13	195		
240	USA, CA	Landers	06/28/1992	RL	7.6 [U]	7.34	114 [5]	71	62	12	744	6.0	2.95
241	USA, CA	Big Bear	06/28/1992	LL	6.7 [U]	6.68	11.6 [5]		20	10	200		
242	USA, Nevada	Little Skull Mtn.	06/29/1992	N	5.4 [U]	5.69	0.38 [5]		8	4.5	36		
243	USA, Oregon	Scotts Mills	03/25/1993	R	5.4 [U]	4.77	0.016 [3]		5.5	9	50		
244	USA, CA	Eureka Valley	05/17/1993	N	5.8 [U]	6.08	1.5 [5]	4.4	16.7	7	117	0.02	

*References for each earthquake are listed in Appendix B.

**RL—right lateral; LL—left lateral; R—reverse; N—normal. For oblique-slip earthquakes, the subordinate sense of slip is listed after the primary slip type.

†Magnitude source listed in brackets: A—Ambraseys, 1975, 1988; B—Abe, 1981; Abe and Noguchi, 1983a, 1983b; C—Lee *et al.*, 1978; D—Duda, 1965, Rothe, 1969; G—Gutenberg and Richter, 1954; I—intensity magnitude; J—Japanese Meteorological Agency; L—Lienkaemper, 1984; m_b—body-wave magnitude; M_L—local or Richter magnitude; PS—M_S Pasadena; PB—Purcaru and Berkhemer, 1982; U—NEIS, USCGS; W—Wu, 1968.

††Source parameters listed in parenthesis are considered unreliable and are not included in any regression analysis.

‡Moment source listed in brackets: 1—estimated from surface length and rupture width using formula $M_0 = \mu A\bar{D}$ (Kanamori and Anderson, 1975), where $\mu = 3 \times 10^{11}$ dyn/cm^2, A = rupture length × rupture width (cm^2), $\bar{D}$ = average displacement on fault (cm); 2—estimated from geodetic modeling of rupture area and displacement using formula $M_0 = \mu A\bar{D}$; 3—measured from surface waves or body waves; 4—averaged from body- and surface-wave measurements; 5—measured from moment tensor solutions.

‡‡Estimated from depths of seismicity on faults.

§Estimated from body- and surface-wave studies.

¶Estimated from geodetic modeling of surface deformation.

#Slemmons, D. B., personal comm., 1989.

Slemmons, 1977; Bonilla *et al.*, 1984). To categorize the dominant slip type for each earthquake in our data base, we use a simple classification scheme based on the ratio of the horizontal component of slip to the vertical component of slip. The horizontal-to-vertical slip ratio is calculated from all estimates of the components of slip, including, in order of priority, surface displacement, geodetic modeling of surface deformation, and the rake from earthquake focal mechanisms.

Published earthquake focal mechanisms were reviewed to compare the nature of surface deformation, such as surface fault displacements and regional subsidence, uplift, or lateral deformation, with the seismologic data for each earthquake. For some earthquakes, there are several published focal mechanisms, including those derived from waveform inversions, *P*-wave first motions, and moment tensor inversions. Because focal mechanisms derived from waveform inversion of long-period *P* and *SH* waves usually are considered more representative of the primary style of co-seismic slip than are short-period *P*-wave first-motion solutions, the former generally are preferred (Aki and Richards, 1980). Theoretically, because the nature and amount of slip at the surface is at least partly controlled by the depth of the focus and the nature of surface geologic conditions, categorizing slip based solely on the slip components measured at the surface may not correspond to the slip type indicated by seismologic data. In practice, however, we find that the dominant sense of slip at the surface is representative of the overall sense of slip measured from the rake of earthquake focal mechanisms.

Slip types for the earthquakes in Table 1 reflect the following scheme, which is based on the ratio of horizontal (HZ; strike slip, S) to vertical (VT; reverse, R, or normal, N) slip:

HZ:VT Slip	>2:1	2:1 to 1:1	1:1 to 1:2	<1:2
Slip Type	S	S-R, S-N	R-S, N-S	R, N

In Table 1, the strike-slip component is characterized as right lateral (RL) or left lateral (LL), depending on the sense of horizontal displacement. For 60 oblique-slip earthquakes, the subordinate sense of slip is listed after the primary slip type. For the regressions, each earthquake is assigned to one of three slip types: strike slip, normal, or reverse. Earthquakes having a horizontal-to-vertical slip ratio greater than 1 to 1 are considered strike slip; those having a horizontal-to-vertical slip ratio of 1 to 1 or less are considered normal or reverse, depending on the sense of vertical displacement.

The earthquakes in Table 1 also are categorized by other characteristics to evaluate potential differences in rupture parameter correlations. Earthquakes are characterized with respect to whether they occurred within a compressional environment (one that is characterized by compressional or transpressional tectonics), or within an extensional environment (one that is characterized by extensional or transtensional tectonics). Slemmons *et al.* (1989) proposed a similar classification for their data base and found no significant differences between regressions developed for the two environments. The earthquakes also are separated according to whether they occurred within an active plate margin or within a stable continental region. Stable continental regions are regions of continental crust that have no significant Cenozoic tectonism or volcanism (Electric Power Research Institute, 1987; Johnston and Kanter, 1990); active plate margins include all other regions in our data base.

Magnitude and Seismic Moment

Estimates of moment magnitude (**M**) and surface-wave magnitude (M_S) are listed in Table 1. Most previous studies of earthquake source parameters compiled M_S estimates, because these are the most commonly cited magnitudes for older instrumental earthquakes. There are, however, several problems associated with using M_S to analyze source parameter relationships. Because M_S is a measure of seismic-wave amplitude at a specific period (approximately 18 to 22 sec), it measures only the energy released at this period. Although M_S values generally are very stable between nearby stations, significant variations in M_S may occur between distant stations. These variations are related to azimuth, station distance, instrument sensitivity, and crustal structure (Panza *et al.*, 1989). Furthermore, for very large earthquakes ($M_S > 8.0$), the periods at which M_S is measured become saturated and no longer record large-scale faulting characteristics (Hanks and Kanamori, 1979). A similar problem with saturation of measured seismic waves also occurs for scales such as local or Richter magnitude (M_L) and body-wave magnitude (m_b). For small earthquakes ($M_S < 5.5$), 20-sec surface-wave amplitudes are too small to be recorded by many seismographs (Kanamori, 1983). Thus, traditional magnitude scales are limited by both the frequency response of the Earth and the response of the recording seismograph.

A physically meaningful link between earthquake size and fault rupture parameters is seismic moment, $M_0 = \mu \bar{D} A$, where μ is the shear modulus [usually taken as 3×10^{11} dyne/cm^2 for crustal faults (Hanks and Kanamori, 1979)]; $\bar{D}$ is the average displacement across the fault surface; and A is the area of the fault surface that ruptured. In turn, M_0 is directly related to magnitude [e.g., $\mathbf{M} = 2/3 * \log M_0 - 10.7$ (Hanks and Kanamori, 1979)].

Seismic moment (M_0) also is considered a more accurate measure of the size of an earthquake than are traditional magnitude scales such as M_S and m_b because it is a direct measure of the amount of radiated energy, rather than a measure of the response of a seismograph to an earthquake (Hanks and Wyss, 1972). It is computed from the source spectra of body and surface waves

(Hanks *et al.*, 1975; Kanamori and Anderson, 1975) or is derived from a moment tensor solution (Dziewonski *et al.*, 1981). Furthermore, there is a larger variability in the value of M_S than of M_0 measured at different stations. For any earthquake, M_S values from stations at different azimuths may differ by as much as 1.5 magnitude units, whereas M_0 values rarely differ by more than a factor of 10, which is equivalent to a variability of 0.7 in **M** values. Thus, **M** is considered a more reliable measure of the energy released during an earthquake (Hanks and Kanamori, 1979).

For earthquakes that lack published M_S estimates, other measures such as Richter magnitude (M_L) or body-wave magnitude (m_b) are listed in Table 1. Because there are several methods for calculating M_S, values calculated by comparable methods are listed where possible. According to Lienkaemper (1984), M_S calculated by the Prague formula, which is used for Preliminary Determination of Epicenters (PDE—U.S. Geological Survey monthly bulletin), is directly comparable to M_{GR} calculated by Gutenberg and Richter (1954). On the average, M_S computed by Abe (1981), Gutenberg (1945), and Richter (1958) differ systematically from M_S (PDE) and M_{GR} (Lienkaemper, 1984). Comparable M_S values listed in this report are taken from the following sources, listed in order of preference: M_S (PDE), M_S (Lienkaemper, 1984), and M_{GR} (Gutenberg and Richter, 1954). Additional sources for magnitudes are listed in the footnotes to Table 1.

To arrive at a single estimate of seismic moment for each earthquake in the data base, we calculate an average seismic moment from all published instrumental seismic moments, including those measured from body waves, surface waves, and centroid moment tensor solutions. Noninstrumental estimates of seismic moment, such as those based on estimates of rupture dimensions or those estimated from magnitude-moment relationships, are not used to calculate average seismic moment. Moment magnitudes are calculated from the averaged seismic moment by the formula of Hanks and Kanamori (1979): $\mathbf{M} = 2/3 * \log M_0 - 10.7$. The values of **M** calculated from M_0 are shown to two decimal places in Table 1 to signify that they are calculated values; these values are used for the regression analyses. When considering individual estimates of moment magnitude, however, these values are considered significant only to one decimal place, and should be rounded to the nearest tenth of a magnitude unit.

Previous studies of the relationship between M_S and **M** indicate that these magnitudes are approximately equal within the range of M_S 5.0 to 7.5 (Kanamori, 1983). Our data set shows no systematic difference between M_S and **M** in the range of magnitude 5.7 to 8.0 (Fig. 1). In the range of magnitude 4.7 to 5.7, M_S is systematically smaller than **M**, in agreement with the results of Boore and Joyner (1982). The standard deviation of the difference between each pair of M_S and **M** values in Figure 1 is approximately 0.19. This standard deviation is less than the standard deviation of 0.28 calculated by Lienkaemper (1984) for residuals of all single-station M_S estimates for individual earthquakes. Based on these standard deviations, the difference between the magnitude scales (M_S and **M**) is insignificant for the earthquakes of magnitude greater than 5.7 listed in Table 1.

For regressions of magnitude versus surface rupture length and magnitude versus maximum displacement, previous studies excluded earthquakes with magnitudes less than approximately M_S 6.0 (Slemmons, 1982; Bonilla *et al.*, 1984; Slemmons *et al.*, 1989). These authors noted that earthquakes of M_S less than 6.0 often have surface ruptures that are much shorter than the source length defined by aftershocks, and that possible surface ruptures for these earthquakes may be less well studied than those for earthquakes of larger magnitude. Furthermore, surface faulting associated with earthquakes of magnitude less than 6.0 may be poorly expressed as discontinuous traces or fractures, showing inconsistent or no net displacement (Darragh and Bolt, 1987; Bonilla, 1988). We evaluate regression statistics for magnitude versus surface rupture length and magnitude versus surface displacement for earthquakes of magnitude less than 6.0 (M_S or **M**), and conclude that elimination of the magnitude cutoff expands the data sets without significantly compromising the regression statistics. Thus, several well-studied surface-rupturing earthquakes of

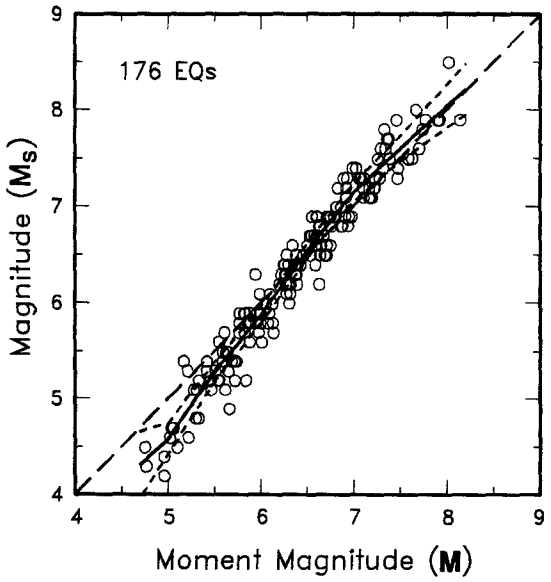

Figure 1. Surface-wave magnitude (M_S) versus moment magnitude (**M**) for historical continental earthquakes. Segmented linear regression shown as solid line, with segment boundaries at **M** 4.7, 5.0, 5.5, 6.0, 6.5, 7.0, 7.5, and 8.2. Short dashed lines indicate 95% confidence interval of regression line. Long dashed line indicates equal magnitudes (1 to 1 slope).

magnitude less than 6.0 (e.g., 1979 Homestead Valley and 1983 Nunez-Coalinga, California) are included in the data base.

For the regressions on subsurface rupture length and on rupture area, the lower bound of magnitude is set at **M** 4.7 because aftershock sequences for earthquakes of lower magnitude rarely are the subject of detailed investigations. Aftershocks and source parameters of numerous recent earthquakes of moderate magnitude (**M** 4.7 to 6.0) have been studied in detail (e.g., 1984 North Wales, England; 1986 Kalamata, Greece; and 1988 Pasadena and 1990 Upland, California). It is appropriate to use these moderate-magnitude earthquakes to evaluate subsurface rupture length, rupture width, and rupture area relationships, because the use of subsurface characteristics eliminates the problems associated with the incomplete expression of rupture at the surface usually associated with moderate-magnitude earthquakes (Darragh and Bolt, 1987).

Instrumentally measured magnitudes (M_S or **M**) do not exist for all the earthquakes listed in Table 1. For these earthquakes, magnitudes are estimated from reports of felt intensity (M_I), or are estimated from the rupture area and displacement using the definition of seismic moment [$M_0 = \mu \bar{D} A$ (Hanks and Kanamori, 1979)]. The earthquakes that lack instrumental magnitudes are included for use in displacement-to-length relationships, which do not require magnitude.

Surface Rupture Length

The length of rupture at the surface is known to be correlatable with earthquake magnitude. This study reviews and reevaluates previously published surface rupture lengths for historical earthquakes and expands the data set to include recent earthquakes and new studies of older events. Published and unpublished descriptions of surface rupture are reviewed to evaluate the nature and extent of surface faulting for 207 earthquakes. Rather than relying on values reported in secondary data compilations, we reviewed original field reports, maps, and articles for each earthquake.

Rupture lengths measured from maps and figures are compared to the lengths reported in descriptions of surface faulting. Descriptions of surface faulting also are reviewed to evaluate whether the ruptures are primary or secondary. Primary surface rupture is defined as being related to tectonic rupture, during which the fault rupture plane intersects the ground surface. Secondary faulting includes fractures formed by ground shaking, fractures and faults related to landslides, and triggered slip on surface faults not related to a primary fault plane (e.g., slip on bedding plane faults or near-surface slip on adjacent or distantly located faults). Because identifying primary tectonic rupture is particularly difficult for smaller-magnitude earthquakes (less than approximately M_S or **M** 6.0), these events are included in regression analyses only when the tectonic nature of the surface rupture is clearly established (e.g., the 1966 Parkfield, California, earthquake, but not the 1986 Chalfant Valley, California, earthquake). Discontinuous surface fractures mapped beyond the ends of the continuous surface trace are considered part of the tectonic surface rupture and are included in the calculation of surface rupture length.

Major sources of uncertainty in reported measurements of surface rupture length are as follows. (1) Incomplete studies of the rupture zone. Less than the entire surface rupture was investigated and mapped for any of various reasons, such as inaccessibility, discontinuity of the surface trace along strike so the entire rupture was not identified, or the fault trace was obscured before postearthquake investigations were undertaken. Considerable uncertainty in the extent of rupture is assessed for investigations completed years to decades after an earthquake. (2) Different interpretations of the nature and extent of surface deformation. Interpretations may differ on the extent of primary surface rupture, the differentiation of primary and secondary surface rupture, and the correlation of surface rupture on different faults to individual earthquakes for multiple event sequences. (3) Unresolvable discrepancies between lengths reported by different workers. These discrepancies are related to level of effort in field investigations, method of measuring fault traces, or lengths reported in text versus the lengths drawn on maps.

Earthquakes are selected for regression analyses involving surface rupture length if the data met all of the following criteria: (1) uncertainty in the rupture length does not exceed approximately 20% of the total length of the rupture; (2) at least one estimate of the amount of surface displacement is reported; and (3) the lengths of ruptures resulting from individual events in multiple earthquake sequences are known.

Subsurface Rupture Length, Downdip Width, and Rupture Area

Subsurface source dimensions, both rupture length and rupture area (length times downdip width), are evaluated for more than 250 earthquakes. Wyss (1979) compiled a smaller data base of rupture areas for continental and subduction zone earthquakes, and Darragh and Bolt (1987) compiled subsurface rupture lengths for moderate-magnitude strike-slip earthquakes. We expand the data base and relate these rupture parameters to moment magnitude.

The primary method used to estimate subsurface rupture length and rupture area is the spatial pattern of early aftershocks. Aftershocks that occur within a few hours to a few days of the mainshock generally define the maximum extent of co-seismic rupture (Kanamori and Anderson, 1975; Dietz and Ellsworth, 1990). Because the distribution of aftershocks may expand laterally and vertically following the mainshock, the initial size of the

aftershock zone is considered more representative of the extent of co-seismic rupture than is the distribution of aftershocks occurring within days to months of the mainshock. Furthermore, detailed studies of aftershocks of several recent earthquakes (such as the 1989 Loma Prieta, California) suggest that early aftershocks occur at the perimeter of the co-seismic rupture zone, and that the central part of this zone is characterized by a lack of seismicity for the first few hours to days after the mainshock (Mendoza and Hartzell, 1988; Dietz and Ellsworth, 1990). This observation suggests that even the rupture area defined by early aftershocks may be slightly larger than the actual co-seismic rupture zone (Mendoza and Hartzell, 1988).

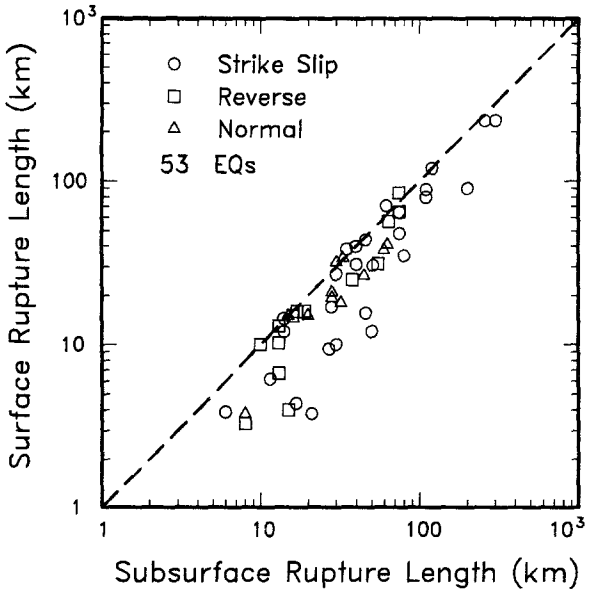

Figure 2. Surface rupture length versus subsurface rupture length estimated from the distribution of early aftershocks of historical continental earthquakes.

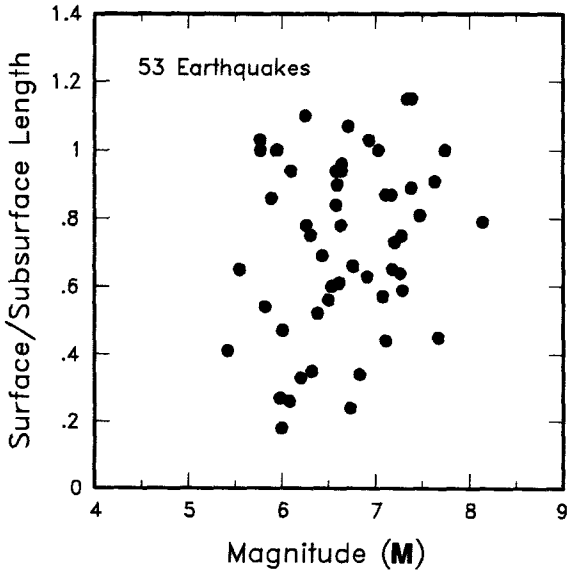

Figure 3. Ratio of surface to subsurface rupture length versus magnitude.

We estimate subsurface rupture length using the length of the best-defined aftershock zone. The accuracy of the size of the aftershock zone depends on the accuracy of the locations of individual aftershocks, which depends, in turn, on the azimuths and proximity of the recording stations and the accuracy of the subsurface structure velocity model. The largest uncertainty typically is incurred in calculating the depths of the hypocenters rather than the areal distribution of epicenters (Gubbins, 1990). Earthquakes are excluded from regression analysis if only a few aftershocks were recorded, or if the aftershock locations were very uncertain.

Alternative but less satisfactory methods to assess the extent of subsurface co-seismic rupture include considering the surface rupture length, geodetic modeling of surface displacement, and modeling of the earthquake source time function. Comparisons for this study suggest that the surface rupture length provides a minimum estimate of the subsurface rupture length. For example, for 53 earthquakes for which data on both surface and subsurface rupture length are available, surface rupture length averaged about 75% of subsurface rupture length (Fig. 2). However, the ratio of surface rupture length to subsurface rupture length appears to increase with magnitude (Fig. 3). Thus, we conclude that surface rupture length is a more reliable estimator of subsurface rupture length as magnitude increases.

Estimates of rupture length calculated from geodetic modeling of vertical and horizontal changes at the ground surface, or from corner frequencies of seismograms (source time functions for circular, unilateral, or bilateral ruptures) also are compiled from the literature. For some earthquakes, rupture lengths estimated from these methods are much shorter than rupture lengths measured from the distribution of aftershocks (Mendoza and Hartzell, 1988). Thus, these measures of rupture length may not represent the extent of co-seismic rupture in the same way that aftershocks do. In this study, estimates of subsurface rupture length based on geodetic modeling or source time functions are accepted for regression analysis only when independent estimates of rupture length are available for corroboration.

Downdip rupture widths are estimated from the depth distribution of the best-defined zone of aftershocks. Where the downdip width of rupture is unknown from the distribution of aftershocks, it is estimated from the depth (thickness) of the seismogenic zone or the depth of the hypocenter and the assumed dip of the fault plane. For most earthquakes of magnitude 5 1/2 or larger, the mainshock typically occurs at or near the base of the seismogenic zone (Sibson, 1987). Estimates of rupture

width based on hypocentral depth of the mainshock or width of the seismogenic zone are used to calculate rupture area only for earthquakes for which detailed information on regional seismicity is available, or for which detailed studies of the hypocentral depth and focal mechanism have been performed.

Major sources of uncertainty for measuring subsurface rupture parameters are as follows: (1) accuracy of aftershock locations in three dimensions; (2) interpretation of the initial extent (length and downdip width) of the aftershock sequence; (3) temporal expansion of the aftershock zone; (4) interpretation of the length of multiple earthquake rupture sequences; (5) identification of the strike and dip of the rupture plane from aftershocks; and (6) reliability of geodetic and seismologic modeling.

Earthquakes are selected for regression analyses involving subsurface rupture length, rupture width, and rupture area if the data met the following criteria: (1) subsurface rupture length and width are measured from an aftershock sequence of known duration; and (2) aftershocks were recorded by a local seismograph network, or many aftershocks were recorded at teleseismic stations. In cases where information on aftershock distribution is lacking, the earthquake is included in the analysis if (1) consistent subsurface rupture lengths are calculated from at least two sources such as geodetic modeling, source time functions, or surface rupture length, and (2) rupture width can be estimated confidently from the thickness of the seismogenic zone or the depth of the mainshock hypocenter.

Maximum and Average Surface Displacement

Observational data from field studies of faults as well as theoretical studies of seismic moment suggest that earthquake magnitude should correlate with the amount of displacement along the causative fault. In contrast to the published information on surface rupture length, displacement measurements for many earthquakes often are poorly documented. In this study, we attempted systematically to compile information on the amount of co-seismic surface displacement and to identify the maximum and the average displacement along the rupture.

The most commonly reported displacement measurement is the *maximum* observed horizontal and/or vertical surface displacement. We reviewed published measurements of displacement, including components of horizontal and vertical slip to calculate a net maximum displacement for each earthquake. Because the majority of displacement measurements reported in the literature were measured weeks to years after the earthquake, these displacement estimates may include post-co-seismic slip or fault creep. For events where displacements were measured at several time periods, we generally select the first measurements recorded after the earthquake to minimize possible effects of fault creep. For several recent events in our data base (such as 1992 Landers, California), we note that little or no postearthquake creep was observed. Thus, displacement measurements recorded several weeks or longer after the earthquake may represent the actual co-seismic slip, except for a few regions where post-co-seismic slip has been documented (e.g., Parkfield and Imperial Valley regions of California).

The net displacement is calculated from the vector sum of the slip components (horizontal and vertical) measured *at a single location*. Commonly, the maximum horizontal displacement and the maximum vertical displacement occur at different locations along a rupture. In those cases, unless the subordinate component is recorded at the sites of the maxima, a net slip vector cannot be calculated. Furthermore, it is difficult to recognize and measure compression and extension across a fault, even for the more recent, well-studied earthquakes.

Average displacement per event is calculated from multiple measurements of displacement along the rupture zone. For most earthquakes, the largest displacements typically occur along a limited reach of the rupture zone. Thus, simple averaging of a limited number of displacement measurements is unlikely to provide an accurate estimate of the true average surface displacement. The most reliable average displacement values are calculated from net displacement measurements recorded along the entire surface rupture. Figure 4 shows a surface displacement distribution for the 1968 Borrego Mountain, California, earthquake, a relatively well-studied event. The average displacement may be calculated by several graphical methods, including a linear point-to-point function, a running three-point average, or an enveloping function that minimizes the effects of anomalously low or high displacement measurements (D. B. Slemmons, 1989, personal comm.). The average-displacement data base reported in this study includes events examined by Slemmons using graphical techniques, and

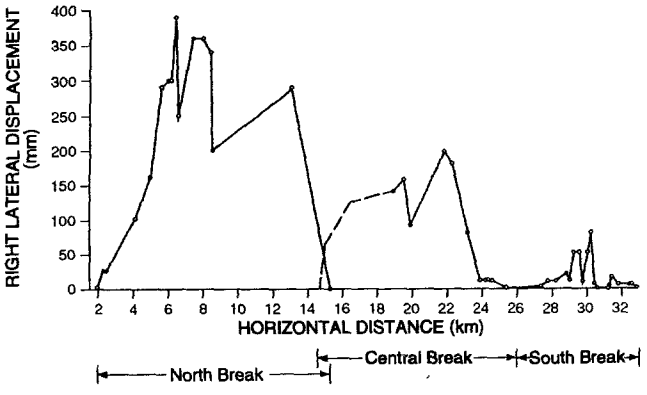

Figure 4. Distribution of right slip measured in April 1968 for the 9 April 1968 Borrego Mountain, California, earthquake. Dashed line indicates estimated displacement for April 1968 (modified from Clark, 1972).

events for which data were obtained from the published literature or calculated from individual measurements of displacement for these earthquakes. Specifically, we include estimates of average displacement that we calculate from a minimum of 10 displacement measurements distributed along the surface rupture, or were reported from extensive studies of the entire surface rupture.

For the average-displacement data set, the maximum surface displacement is about twice the average surface displacement, although the ratio of average to maximum surface displacement ranges from about 0.2 to 0.8 (Fig. 5). In addition, for a subset of earthquakes with published instrumental estimates of seismic moment, the ratio of average to maximum displacement does not vary systematically as a function of magnitude (Fig. 5).

A matter of interest is the relationship of co-seismic surface displacement to "subsurface" displacement that occurs on the fault plane within the seismogenic crust (as given in the definition of seismic moment). To evaluate the relationship of surface displacement to average subsurface displacement, we calculate an average displacement from the seismic moment and the rupture area for all earthquakes having acceptable estimates of maximum and average surface displacement, seismic moment, and rupture area. The calculated values of subsurface displacement are compared with the observed maximum and average surface displacements in Figures 6 and 7. The ratio of average subsurface displacement to maximum surface displacement ranges from 0.14 to 7.5; the ratio of average subsurface displacement to average surface displacement ranges from 0.25 to 6.0. These ratios do not appear to vary as a function of magnitude (Figs. 6a and 6b).

To evaluate the distribution of data, we calculate residuals for the ratios and find that the distribution is consistent with a normal distribution of data. Because of this and because of the large range of data, we believe that the mode provides an appropriate measure of the distribution of ratios. For 44 earthquakes for which we have estimates of both maximum displacement and subsurface displacement, the mode of the distribution of the ratios of average subsurface displacement to maximum surface displacement is 0.76 (Fig. 7a). This indicates that for most earthquakes, the average subsurface displacement is less than the maximum surface displacement. For 32 earthquakes for which we have estimates of both average displacement and subsurface displacement, the mode of the distribution of the ratios of average subsurface displacement to average surface displacement is 1.32 (Fig. 7b). Thus, for the earthquakes in our data set, average subsurface displacement is more than average surface displacement and less than maximum surface displacement. Furthermore, for these earthquakes, most slip on the fault plane at seismogenic depths is manifested at the surface.

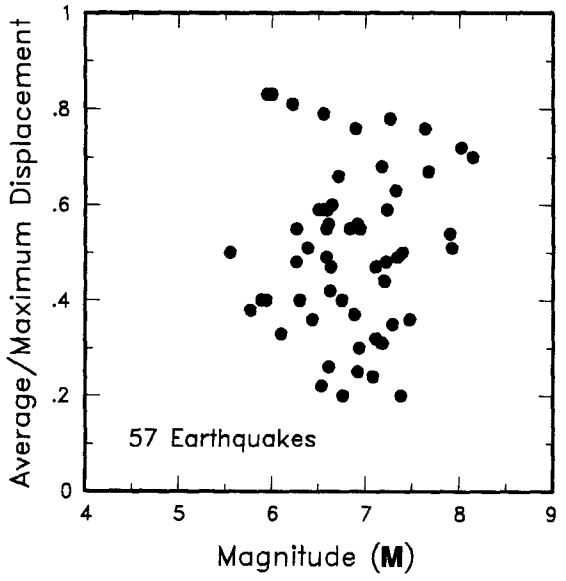

Figure 5. Ratio of average surface to maximum surface displacement versus magnitude.

The major sources of uncertainty in the displacement data set reflect the following: (1) documentation of less than the entire fault rupture trace; (2) lack of suitable features (e.g., stratigraphy, streams, or cultural features) for measuring displacement; (3) distribution of displacement along multiple fault strands, or distributed shearing over a broad fault zone; (4) modification of the fault scarp by landsliding or erosion; (5) increase in displacement due to afterslip; (6) inadequately documented locations of slip measurements; and (8) measurements of slip on geomorphic features displaced by repeated earthquakes or postearthquake creep.

Earthquakes are selected for regression analyses involving displacement if the data met all of the following criteria: (1) type of displacement (strike slip, reverse, normal) and nature of measurement (maximum or average surface slip) are known; (2) slip occurred primarily on a single fault, or the total slip across a zone of faults is known; (3) net maximum displacement is calculated from horizontal and vertical components of slip measured at a single locality; and (4) the measured displacement can be attributed uniquely to the most recent earthquake. In addition, for average displacement, the estimate is calculated from the sum of numerous contemporaneous displacement measurements, or was reported in literature by researchers who investigated the entire length of the surface rupture.

Regression Models

Numerous regression models exist for evaluating the relationship between any pair of variables, including models for linear or nonlinear relationships and normal (Gaussian) or nonparametric distributions of data. Most previous studies of fault rupture parameters used a sim-

ple linear regression model such as ordinary least squares. Other models considered for this study included least-normal squares and reduced major axis (Troutman and Williams, 1987). These models have the advantage of providing a unique solution regardless of which variable is chosen to be the dependent variable. Although this unique solution provides the best fit to all the data, and thus the most accurate interpretation of the relationship between variables, it does not minimize the error in predicting any individual variable. An ordinary least-squares model, however, calculates a nonunique solution that minimizes the error in predicting the dependent variable from the independent variable (Troutman and Williams, 1987). Thus, because we are interested in predicting parameters to evaluate seismic hazard, and to make our new empirical relationships comparable to previously determined relationships, we use an ordinary least-squares regression model for all analyses.

A further consideration in selecting a regression model is how it treats uncertainties in the data. Based on their detailed analysis of the "measurement" uncertainties associated with magnitudes (M_S), surface rupture lengths, and maximum displacements, Bonilla *et al.* (1984) noted that for any given earthquake, the stochastic variance (earthquake-to-earthquake differences) in these rupture parameters dominates errors in measurement. Specifi-

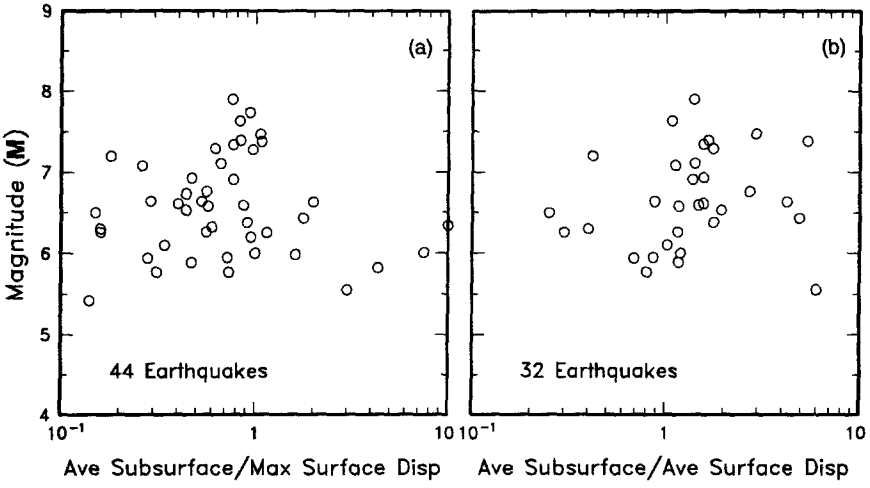

Figure 6. (a) Ratio of average subsurface to maximum surface displacement versus magnitude. (b) Ratio of average subsurface to average surface displacement versus magnitude. Average subsurface displacement is calculated from the seismic moment and the rupture area.

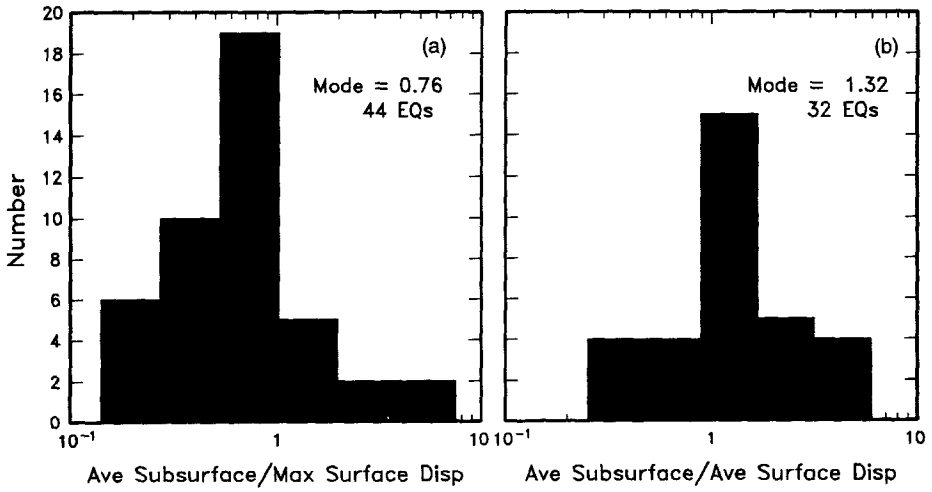

Figure 7. (a) Histogram of the logarithm of the ratio of average subsurface to maximum surface displacement. (b) Histogram of the logarithm of the ratio of average subsurface to average surface displacement. Average subsurface displacement is calculated from the seismic moment and the rupture area.

cally, they observed that a weighted least-squares model, which incorporates estimated measurement errors as a weighing factor, provides no better correlations than does an ordinary least-squares regression model. Similarly, Singh *et al.* (1980) analyzed the effects of data errors on solutions from linear and quadratic regressions. They concluded that there are significant difficulties in estimating the errors in source parameters, and that including estimated errors did not significantly improve the statistical correlations.

Although earthquake-specific uncertainties in the measured data are not listed in Table 1, the uncertainty in each listed parameter falls within the limits of acceptability defined by the selection criteria, except for those parameters shown in parentheses. The parameters shown in parenthesis are excluded from the regression analyses because the uncertainties in the values are too large; however, these values are included in the data set for the sake of completeness. Thus, we consider the measurement uncertainties during the data selection process, but not for the regression analyses. For the 244 earthquakes included in the analyses, the uncertainties in measurements for any given earthquake are considered much smaller than the stochastic variation in the data set as a whole.

One assumption of ordinary least-squares models is that the residuals have a normal distribution. Because many geologic and seismologic variables do not have a normal distribution, it is necessary to transform the data to a logarithmic form; this transformed data typically has a normal distribution (Davis, 1986). To test the assumption that the data sets have a (log) normal distribution, we calculate residuals between the empirical data and the predicted independent variable from each regression equation. We complete X^2 tests for binned and unbinned data sets for each set of residuals. We compute the optimum number of bins for each data set using the method of Benjamin and Cornell (1970). The X^2 tests indicate that the distribution of residuals for all data sets is consistent with a normal distribution of data at a 95% significance level. We also examine the distribution of residuals for each data set to evaluate the fit of the data to the regression model. Because the distribution of residuals shows no obvious trends, a linear regression model provides a satisfactory fit to the data (Fig. 8).

One significant change from the methods and results of most previous studies is that our analyses present regressions based on moment magnitude (**M**) rather than surface-wave magnitude (M_S). During preliminary analysis of the regression relationships, we observed that the standard deviation of magnitude is consistently smaller for relationships based on **M** than for relationships based on M_S. In addition, the correlation coefficient generally is slightly higher for **M** relationships than for M_S relationships. One advantage, however, to using M_S-based relationships is that the number of events in each relationship is increased. We consider the smaller standard deviations and generally improved correlations for **M**-based relationships more important than increasing the size of the data set. We present only regressions based on **M**; for different applications, however, M_S-based relationships may be calculated from the data set.

Regression Results and Statistical Significance

Ordinary least-squares regression analyses (Tables 2A and 2B) include regression of **M** and $\log_{10}$ of surface rupture length, subsurface rupture length, downdip rupture width, rupture area, maximum surface displacement, and average surface displacement as a function of

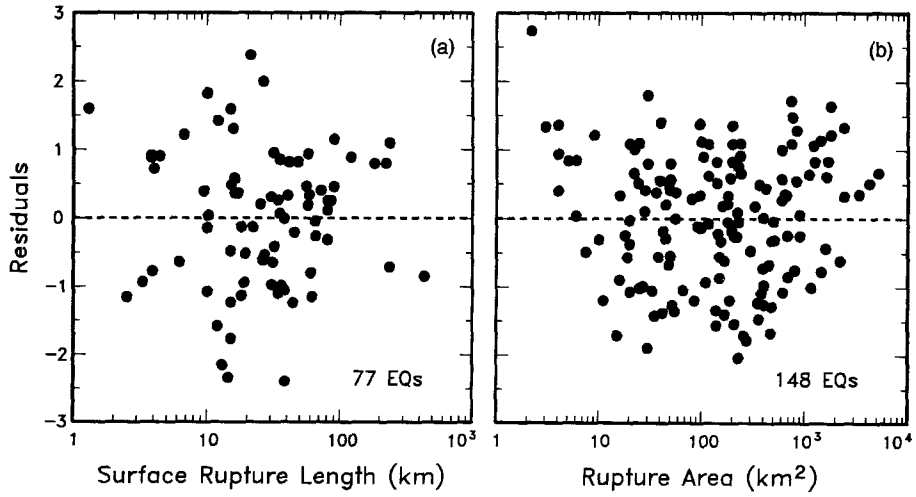

Figure 8. (a) Residuals for surface rupture length regression versus observed surface rupture length. (b) Residuals for rupture area regression versus observed rupture area.

slip type. Regressions of surface rupture length and maximum and average displacement also are presented (Table 2C). Regression descriptors include number of events, regression coefficients (a and b), standard error of the coefficients, standard deviation of the dependent variable (s), correlation coefficient (r), and data range. The empirical relationships have the form $y = a + b * \log(x)$ or $\log(y) = a + b * \log(x)$, where y is the dependent variable and x is the independent variable. Two plots are presented for each pair of parameters. The first shows the data, the "all-slip-type" regression line (i.e., the regression fit to all of the data), and the 95% confidence interval (Figs. 9a through 16a). The second shows the regression lines for individual slip types (Figures 9b through 16b). The length of the regression line shows the range of data for each empirical relationship.

We calculate t statistics for the correlation coefficient to evaluate the significance of each relationship. A t distribution estimates a probability distribution based on the size of the data set. We use a t test to calculate critical values of t, then compare these values to critical values of t for a selected significance level. We evaluate significance levels for a two-tailed distribution, because the correlation may be positive or negative. All relationships are significant at a 95% probability level, except for the reverse-slip relationships for maximum and average displacement. These relationships are not significant because the position of the regression line is poorly constrained by the data; they are shown in brackets in Table 2 because they are not considered useful for predicting dependent variables. Furthermore, we exclude them from comparisons to regression lines for other relationships. The results of our analyses indicate a poor correlation between surface displacement and other rupture parameters for reverse-slip earthquakes. The reverse-slip relationships excluded from further analysis include maximum displacement versus magnitude, average displacement versus magnitude, surface rupture

Table 2A
Regressions of Rupture Length, Rupture Width, Rupture Area, and Moment Magnitude (M)

Equation*	Slip Type†	Number of Events	Coefficients and Standard Errors		Standard Deviation	Correlation Coefficient	Magnitude Range	Length/Width Range (km)
			a(sa)	b(sb)	s	r		
$\mathbf{M} = a + b * \log(\mathrm{SRL})$	SS	43	5.16(0.13)	1.12(0.08)	0.28	0.91	5.6 to 8.1	1.3 to 432
	R	19	5.00(0.22)	1.22(0.16)	0.28	0.88	5.4 to 7.4	3.3 to 85
	N	15	4.86(0.34)	1.32(0.26)	0.34	0.81	5.2 to 7.3	2.5 to 41
	All	77	5.08(0.10)	1.16(0.07)	0.28	0.89	5.2 to 8.1	1.3 to 432
$\log(\mathrm{SRL}) = a + b * \mathbf{M}$	SS	43	−3.55(0.37)	0.74(0.05)	0.23	0.91	5.6 to 8.1	1.3 to 432
	R	19	−2.86(0.55)	0.63(0.08)	0.20	0.88	5.4 to 7.4	3.3 to 85
	N	15	−2.01(0.65)	0.50(0.10)	0.21	0.81	5.2 to 7.3	2.5 to 41
	All	77	−3.22(0.27)	0.69(0.04)	0.22	0.89	5.2 to 8.1	1.3 to 432
$\mathbf{M} = a + b * \log(\mathrm{RLD})$	SS	93	4.33(0.06)	1.49(0.05)	0.24	0.96	4.8 to 8.1	1.5 to 350
	R	50	4.49(0.11)	1.49(0.09)	0.26	0.93	4.8 to 7.6	1.1 to 80
	N	24	4.34(0.23)	1.54(0.18)	0.31	0.88	5.2 to 7.3	3.8 to 63
	All	167	4.38(0.06)	1.49(0.04)	0.26	0.94	4.8 to 8.1	1.1 to 350
$\log(\mathrm{RLD}) = a + b * \mathbf{M}$	SS	93	−2.57(0.12)	0.62(0.02)	0.15	0.96	4.8 to 8.1	1.5 to 350
	R	50	−2.42(0.21)	0.58(0.03)	0.16	0.93	4.8 to 7.6	1.1 to 80
	N	24	−1.88(0.37)	0.50(0.06)	0.17	0.88	5.2 to 7.3	3.8 to 63
	All	167	−2.44(0.11)	0.59(0.02)	0.16	0.94	4.8 to 8.1	1.1 to 350
$\mathbf{M} = a + b * \log(\mathrm{RW})$	SS	87	3.80(0.17)	2.59(0.18)	0.45	0.84	4.8 to 8.1	1.5 to 350
	R	43	4.37(0.16)	1.95(0.15)	0.32	0.90	4.8 to 7.6	1.1 to 80
	N	23	4.04(0.29)	2.11(0.28)	0.31	0.86	5.2 to 7.3	3.8 to 63
	All	153	4.06(0.11)	2.25(0.12)	0.41	0.84	4.8 to 8.1	1.1 to 350
$\log(\mathrm{RW}) = a + b * \mathbf{M}$	SS	87	−0.76(0.12)	0.27(0.02)	0.14	0.84	4.8 to 8.1	1.5 to 350
	R	43	−1.61(0.20)	0.41(0.03)	0.15	0.90	4.8 to 7.6	1.1 to 80
	N	23	−1.14(0.28)	0.35(0.05)	0.12	0.86	5.2 to 7.3	3.8 to 63
	All	153	−1.01(0.10)	0.32(0.02)	0.15	0.84	4.8 to 8.1	1.1 to 350
$\mathbf{M} = a + b * \log(\mathrm{RA})$	SS	83	3.98(0.07)	1.02(0.03)	0.23	0.96	4.8 to 7.9	3 to 5,184
	R	43	4.33(0.12)	0.90(0.05)	0.25	0.94	4.8 to 7.6	2.2 to 2,400
	N	22	3.93(0.23)	1.02(0.10)	0.25	0.92	5.2 to 7.3	19 to 900
	All	148	4.07(0.06)	0.98(0.03)	0.24	0.95	4.8 to 7.9	2.2 to 5,184
$\log(\mathrm{RA}) = a + b * \mathbf{M}$	SS	83	−3.42(0.18)	0.90(0.03)	0.22	0.96	4.8 to 7.9	3 to 5,184
	R	43	−3.99(0.36)	0.98(0.06)	0.26	0.94	4.8 to 7.6	2.2 to 2,400
	N	22	−2.87(0.50)	0.82(0.08)	0.22	0.92	5.2 to 7.3	19 to 900
	All	148	−3.49(0.16)	0.91(0.03)	0.24	0.95	4.8 to 7.9	2.2 to 5,184

*SRL—surface rupture length (km); RLD—subsurface rupture length (km); RW—downdip rupture width (km), RA—rupture area (km^2).
†SS—strike slip; R—reverse; N—normal.

length versus maximum displacement, and surface rupture length versus average displacement. We also evaluate regressions between M_S and displacement; we observe similar trends in correlation coefficients and standard deviations for each slip type.

Analysis of Parameter Correlations

The empirical regressions for all-slip-type relationships (Table 2) as well as the data plots (Figs. 9a through 16a) enable us to evaluate the correlations among various rupture parameters. The strongest correlations (r = 0.89 to 0.95) exist between magnitude (**M**) and surface rupture length, subsurface rupture length, and rupture area. These regressions also have the lowest standard deviations (s = 0.24 to 0.28 magnitude units). Magnitude versus displacement relationships have lower correlations (r = 0.75 to 0.78) and higher standard deviations (s = 0.39 to 0.40 magnitude units). Displacement versus length relationships have the weakest correlation (r = 0.71 to 0.75), with standard deviations of 0.36 to 0.41 magnitude units. These results indicate that displacement and rupture length generally correlate better with magnitude than with each other. The weaker correlations may reflect the wide range of displacement values (variations as great as 1 1/4 orders of magnitude) observed for ruptures of the same length (Figs. 12a and 13a).

In general, the relatively high correlations ($r > 0.7$) and low standard deviations for all the regressions indicate there is a strong correlation among the various rupture parameters, and that these regressions may be used confidently to estimate dependent variables.

Because our relationships are based on **M** rather than M_S, a quantitative comparison with most regressions calculated for previous studies cannot be made. For the surface rupture length and maximum displacement regressions based on M_S that we calculated during our preliminary analyses, we observed that the correlation coefficients generally were slightly higher, and the standard deviations were lower, than for the regressions calculated by Bonilla *et al.* (1984), Slemmons (1982), Slemmons *et al.* (1989), and Wesnousky (1986). We also observed that our regressions typically provided similar magnitude estimates to the relationships of Slemmons, and slightly lower magnitude estimates than the relationships of Bonilla *et al.* (1984). The coefficients for our all-slip-type rupture area regression are similar to the coefficients estimated by Wyss (1979) for an **M** versus rupture area relationship. Further, because the data sets we use to calculate regressions typically are much larger than the data sets used for previous studies, even qualitative comparisons among results of different studies are difficult to evaluate.

Effects of Slip Type on Regressions

By comparing the regressions for various slip types (Figs. 9b through 16b), we may evaluate the differences in magnitude or displacement that will result from a given fault parameter as a function of the sense of slip. The sensitivity of the regressions to the sense of slip greatly affects their application, because estimating the sense of slip of a fault may be difficult. If the regressions are insensitive to slip type, such a determination would be unnecessary, and using the all-slip-type regression would be appropriate. A further advantage to using all-slip-type

Table 2B
Regressions of Displacement and Moment Magnitude (**M**)

Equation*	Slip Type†	Number of Events	Coefficients and Standard Errors		Standard Deviation	Correlation Coefficient	Magnitude Range	Displacement Range (km)
			a(sa)	b(sb)	s	r		
M = a + b * log (MD)	SS	43	6.81(0.05)	0.78(0.06)	0.29	0.90	5.6 to 8.1	0.01 to 14.6
	{*R*‡	*21*	*6.52(0.11)*	*0.44(0.26)*	*0.52*	*0.36*	*5.4 to 7.4*	*0.11 to 6.5*}
	N	16	6.61(0.09)	0.71(0.15)	0.34	0.80	5.2 to 7.3	0.06 to 6.1
	All	80	6.69(0.04)	0.74(0.07)	0.40	0.78	5.2 to 8.1	0.01 to 14.6
log (MD) = a + b * **M**	SS	43	−7.03(0.55)	1.03(0.08)	0.34	0.90	5.6 to 8.1	0.01 to 14.6
	{*R*	*21*	*−1.84(1.14)*	*0.29(0.17)*	*0.42*	*0.36*	*5.4 to 7.4*	*0.11 to 6.5*}
	N	16	−5.90(1.18)	0.89(0.18)	0.38	0.80	5.2 to 7.3	0.06 to 6.1
	All	80	−5.46(0.51)	0.82(0.08)	0.42	0.78	5.2 to 8.1	0.01 to 14.6
M = a + b * log (AD)	SS	29	7.04(0.05)	0.89(0.09)	0.28	0.89	5.6 to 8.1	0.05 to 8.0
	{*R*	*15*	*6.64(0.16)*	*0.13(0.36)*	*0.50*	*0.10*	*5.8 to 7.4*	*0.06 to 1.5*}
	N	12	6.78(0.12)	0.65(0.25)	0.33	0.64	6.0 to 7.3	0.08 to 2.1
	All	56	6.93(0.05)	0.82(0.10)	0.39	0.75	5.6 to 8.1	0.05 to 8.0
log (AD) = a + b * **M**	SS	29	−6.32(0.61)	0.90(0.09)	0.28	0.89	5.6 to 8.1	0.05 to 8.0
	{*R*	*15*	*−0.74(1.40)*	*0.08(0.21)*	*0.38*	*0.10*	*5.8 to 7.4*	*0.06 to 1.5*}
	N	12	−4.45(1.59)	0.63(0.24)	0.33	0.64	6.0 to 7.3	0.08 to 2.1
	All	56	−4.80(0.57)	0.69(0.08)	0.36	0.75	5.6 to 8.1	0.05 to 8.0

*MD—maximum displacement (m); AD—average displacement (M).
†SS—strike slip; R—reverse; N—normal.
‡Regressions for reverse-slip relationships shown in italics and brackets are not significant at a 95% probability level.

Table 2C
Regressions of Surface Rupture Length and Displacement

Equation*	Slip Type†	Number of Events	Coefficients and Standard Errors a(sa)	b(sb)	Standard Deviation s	Correlation Coefficient r	Displacement Range (m)	Rupture Length Range (km)
log (MD) = a + b * log (SRL)	SS	55	−1.69(0.16)	1.16(0.09)	0.36	0.86	0.01 to 14.6	1.3 to 432
	{R‡	*21*	*−0.44(0.34)*	*0.42(0.23)*	*0.43*	*0.38*	*0.11 to 6.5*	*4 to 148*}
	N	19	−1.98(0.50)	1.51(0.35)	0.41	0.73	0.06 to 6.4	3.8 to 75
	All	95	−1.38(0.15)	1.02(0.09)	0.41	0.75	0.01 to 14.6	1.3 to 432
log (SRL) = a + b * log (MD)	SS	55	1.49(0.04)	0.64(0.05)	0.27	0.86	0.01 to 14.6	1.3 to 432
	{R	*21*	*1.36(0.09)*	*0.35(0.19)*	*0.39*	*0.38*	*0.11 to 6.5*	*4 to 148*}
	N	19	1.36(0.05)	0.35(0.08)	0.20	0.73	0.06 to 6.4	3.8 to 75
	All	95	1.43(0.03)	0.56(0.05)	0.31	0.75	0.01 to 14.6	1.3 to 432
log (AD) = a + b * log (SRL)	SS	35	−1.70(0.23)	1.04(0.13)	0.32	0.82	0.10 to 8.0	3.8 to 432
	{R	*17*	*−0.60(0.39)*	*0.31(0.27)*	*0.40*	*0.28*	*0.06 to 2.6*	*6.7 to 148*}
	N	14	−1.99(0.72)	1.24(0.49)	0.37	0.59	0.08 to 2.1	15 to 75
	All	66	−1.43(0.18)	0.88(0.11)	0.36	0.71	0.06 to 8.0	3.8 to 432
log (SRL) = a + b * log (AD)	SS	35	1.68(0.04)	0.65(0.08)	0.26	0.82	0.10 to 8.0	3.8 to 432
	{R	*17*	*1.45(0.10)*	*0.26(0.23)*	*0.36*	*0.28*	*0.06 to 2.6*	*6.7 to 148*}
	N	14	1.52(0.05)	0.28(0.11)	0.17	0.59	0.08 to 2.1	15 to 75
	All	66	1.61(0.04)	0.57(0.07)	0.29	0.71	0.06 to 8.0	3.8 to 432

*SRL—surface rupture length (km); MD—maximum displacement (m); AD—average displacement (m).
§SS—strike slip; R—reverse; N—normal.
‡Regressions for reverse-slip relationships shown in italics and brackets are not significant at a 95% probability level.

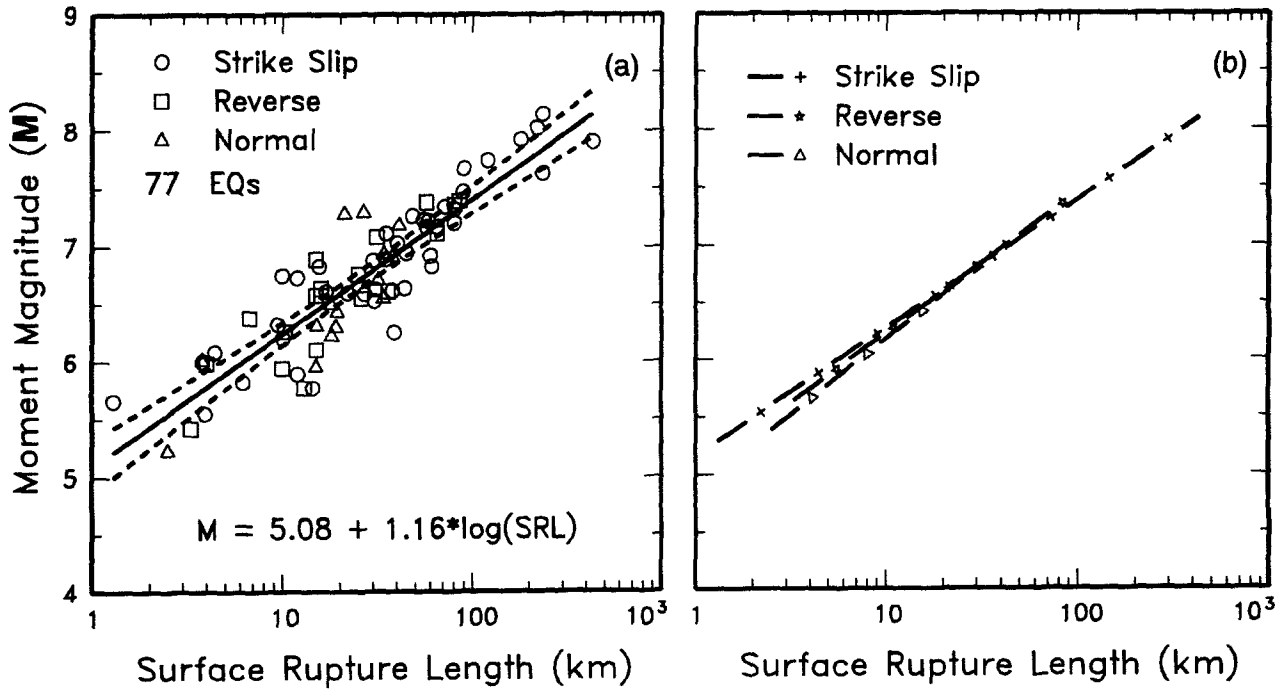

Figure 9. (a) Regression of surface rupture length on magnitude (**M**). Regression line shown for all-slip-type relationship. Short dashed line indicates 95% confidence interval. (b) Regression lines for strike-slip, reverse, and normal-slip relationships. See Table 2 for regression coefficients. Length of regression lines shows the range of data for each relationship.

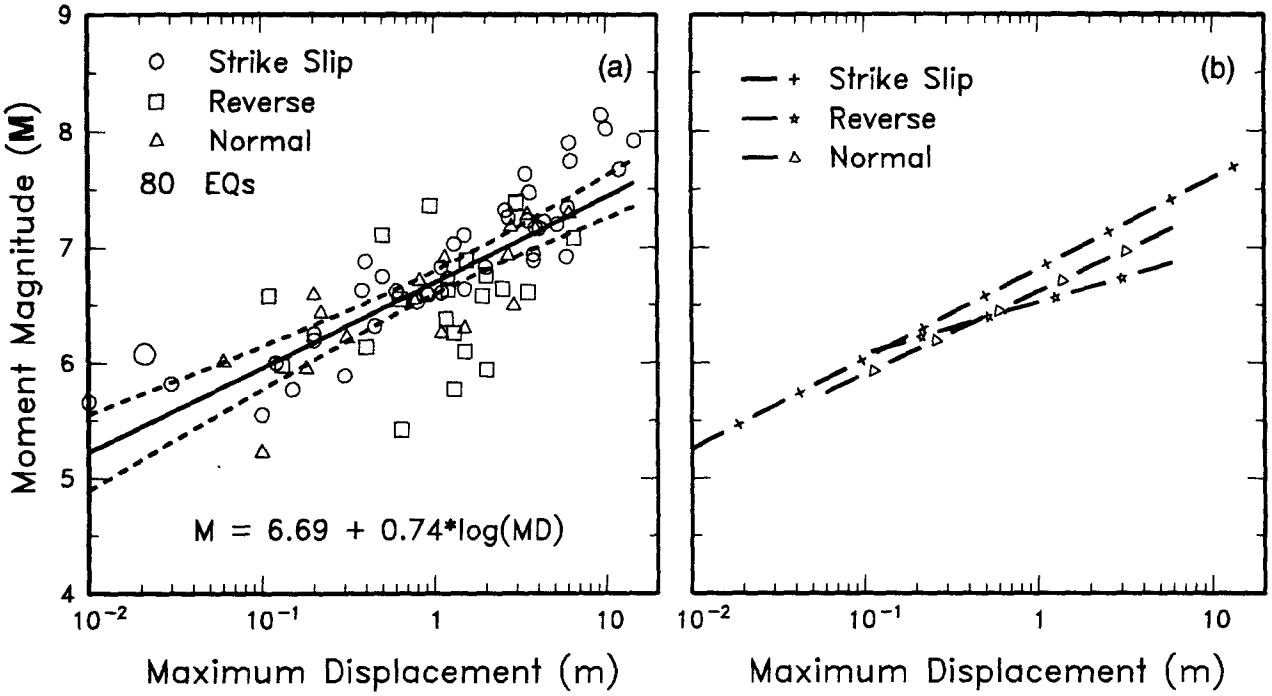

Figure 10. (a) Regression of maximum surface displacement on magnitude (**M**). Regression line shown for all-slip-type relationship. Short dashed line indicates 95% confidence interval. (b) Regression lines for strike-slip, reverse, and normal-slip relationships. See Table 2 for regression coefficients. Length of regression lines shows the range of data for each relationship.

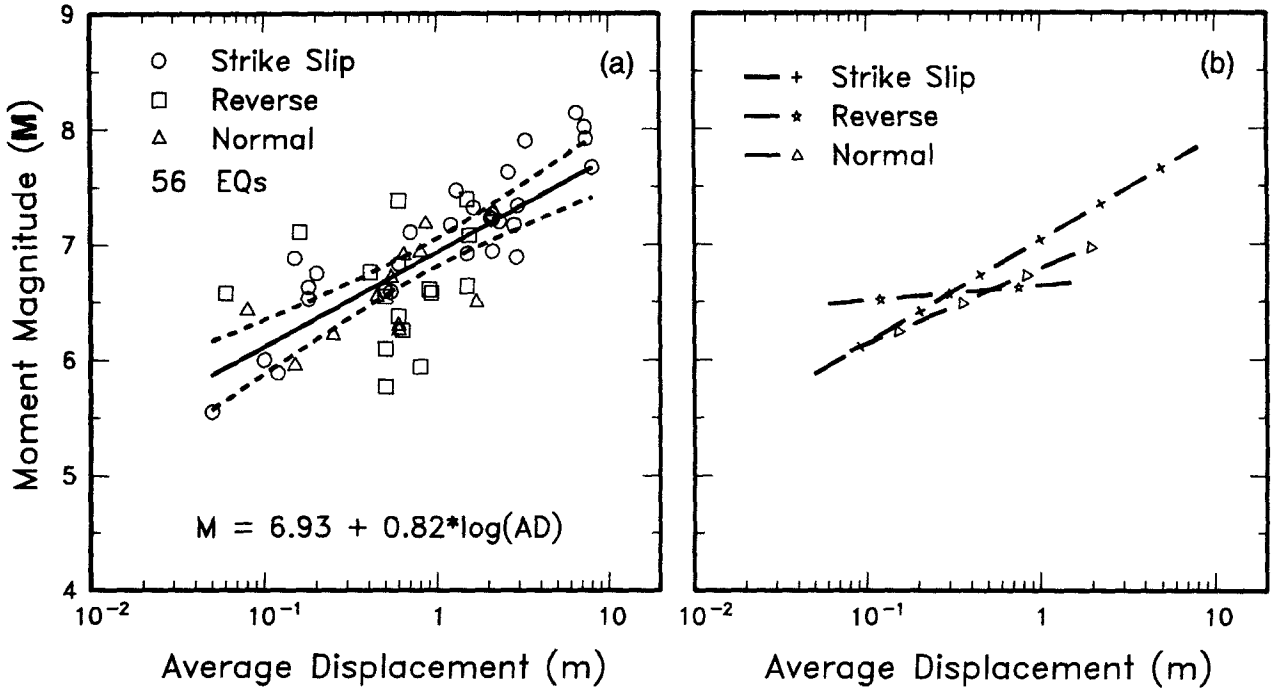

Figure 11. (a) Regression of average surface displacement on magnitude (**M**). Regression line shown for all-slip-type relationship. Short dashed line indicates 95% confidence interval. (b) Regression lines for strike-slip, reverse, and normal-slip relationships. See Table 2 for regression coefficients. Length of regression lines shows the range of data for each relationship.

regressions is that the range of application for the regressions is larger than for single-slip type regressions.

Visually, there is little difference in the position of the regression lines as a function of the sense of slip for surface rupture length, subsurface rupture length, or rupture area (Figs. 9b, 15b, and 16b). Other relationships show larger differences between the position of the regression lines (Figs. 10b through 14b). To evaluate the statistical significance of the differences in the results, we use *t* statistics to compare the regression coefficients for individual slip-type data sets to the coefficients for the rest of the data (i.e., SS to N + R, N to R + SS, and R to SS + N). We also evaluate individual slip relationships to each other (SS to R, SS to N, R to N). We use the statistical analysis to evaluate whether regression coefficients differ at high levels of significance (generally 95%). In some cases, as discussed below, we examine the coefficients at higher levels of significance (e.g., 99%). In the following discussion, the difference between regression coefficients is considered negligible if they are not different at a 95% significance level. The difference between regression coefficients becomes appreciable if they are different at higher levels of significance.

We observe no difference as a function of slip type at a 95% significance level (i.e., the regression coefficients do not differ at a 95% significance level) for relationships between surface rupture length and magnitude and subsurface rupture length and magnitude. For these relationships, using the all-slip-type relationship is appropriate because it eliminates the need to assess the type of fault slip. Furthermore, the uncertainty in the mean is smaller for the all-slip-type relationship than for any individual slip-type regression, because the data set is much larger.

For rupture area versus magnitude, we observe no difference in the coefficients of strike slip and normal regressions at a 95% significance level. The reverse regression coefficients differ from normal and strike-slip coefficients at all levels of significance. For downdip rupture width versus magnitude, the coefficients of reverse and strike-slip regressions differ at all levels of significance. Normal and strike-slip coefficients, and reverse and normal coefficients do not differ at 95 to 98% significance. These results indicate that the reverse-slip regression may be most appropriate for estimating magnitude, rupture width, or rupture area for reverse-slip faults, whereas the all-slip-type regression may be appropriate for other fault types.

We note, however, that even though the regression coefficients may differ at various levels of significance, the actual difference between the expected magnitudes that the regressions provide typically is very small. For example, for an expected rupture area of 100 km^2, strike-

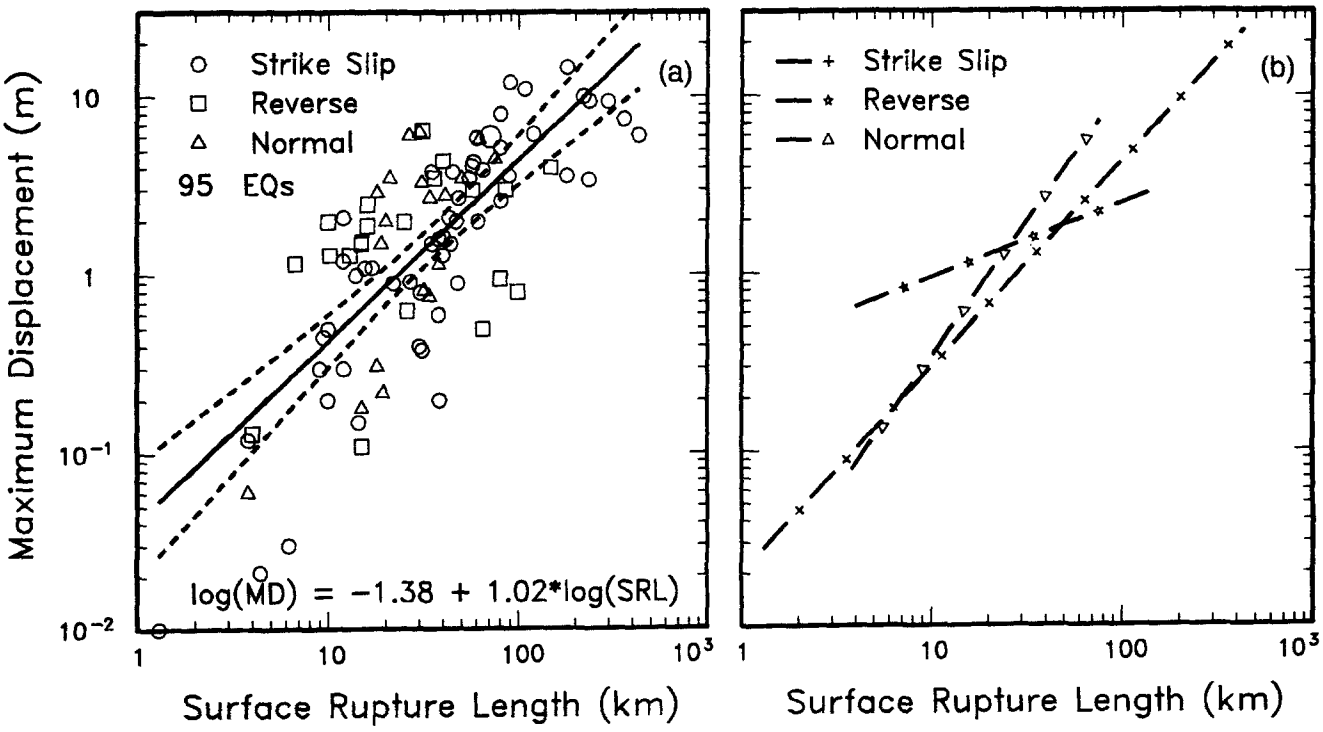

Figure 12. (a) Regression of surface rupture length on maximum displacement. Regression line shown for all-slip-type relationship. Short dashed line indicates 95% confidence interval. (b) Regression lines for strike-slip, reverse, and normal-slip relationships. See Table 2 for regression coefficients. Length of regression lines shows the range of data for each relationship.

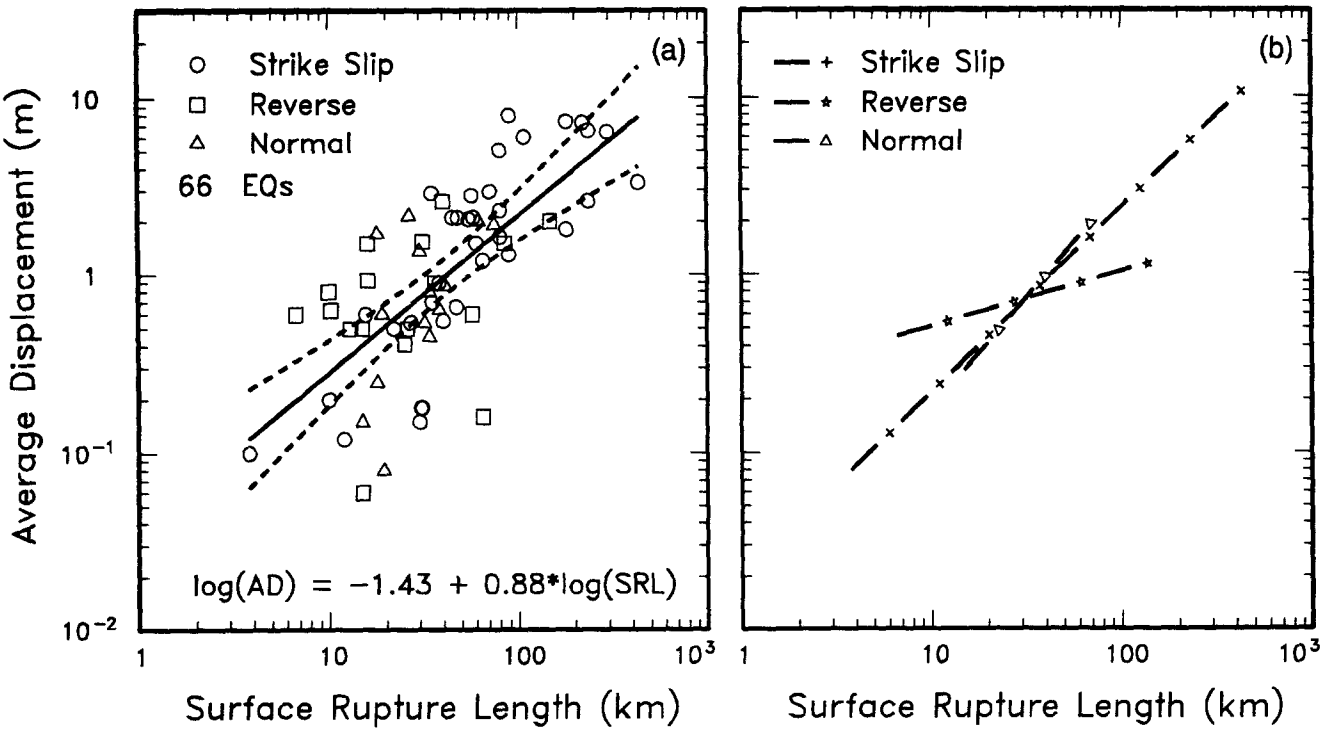

Figure 13. (a) Regression of surface rupture length on average displacement. Regression line shown for all-slip-type relationship. Short dashed line indicates 95% confidence interval. (b) Regression lines for strike-slip, reverse, and normal-slip relationships. See Table 2 for regression coefficients. Length of regression lines shows the range of data for each relationship.

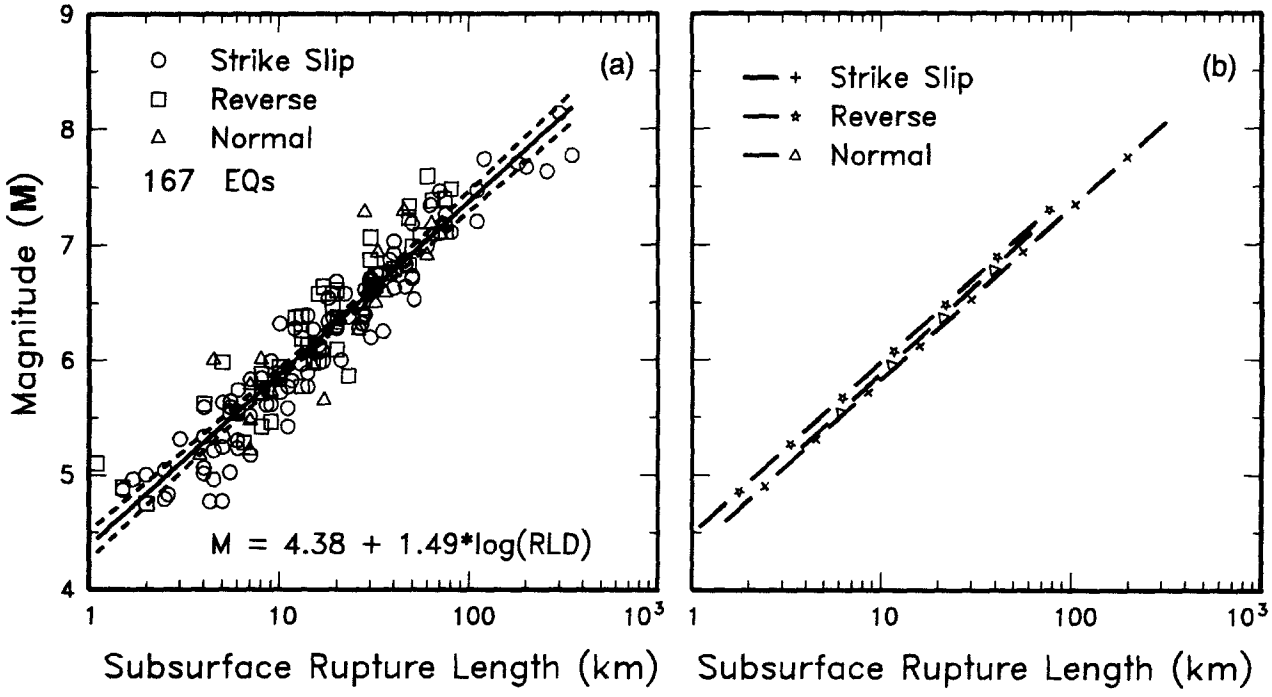

Figure 14. (a) Regression of subsurface rupture length on magnitude (**M**). Regression line shown for all-slip-type relationship. Short dashed line indicates 95% confidence interval. (b) Regression lines for strike-slip relationships. See Table 2 for regression coefficients. Length of regression lines shows the range of data for each relationship.

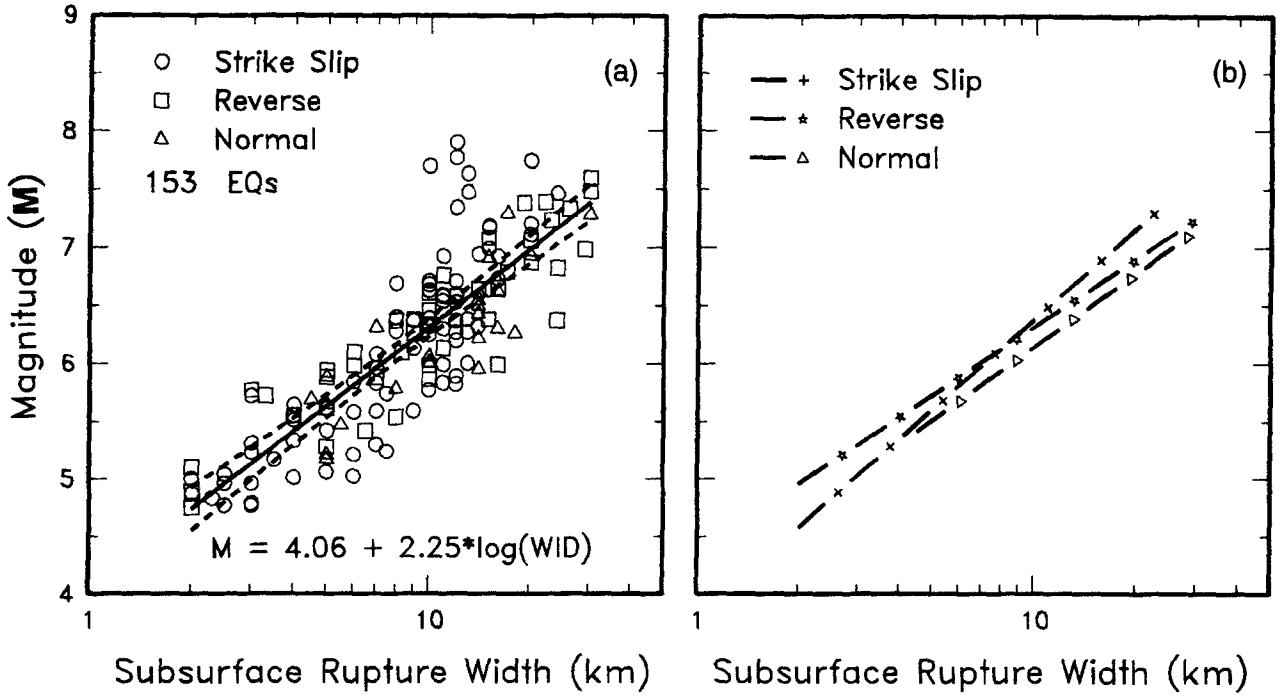

Figure 15. (a) Regression of downdip rupture width on magnitude (M). Regression line shown for all-slip-type relationship. Short dashed line indicates 95% confidence interval. (b) Regression lines for strike-slip, reverse, and normal-slip relationships. See Table 2 for regression coefficients. Length of regression lines shows the range of data for each relationship.

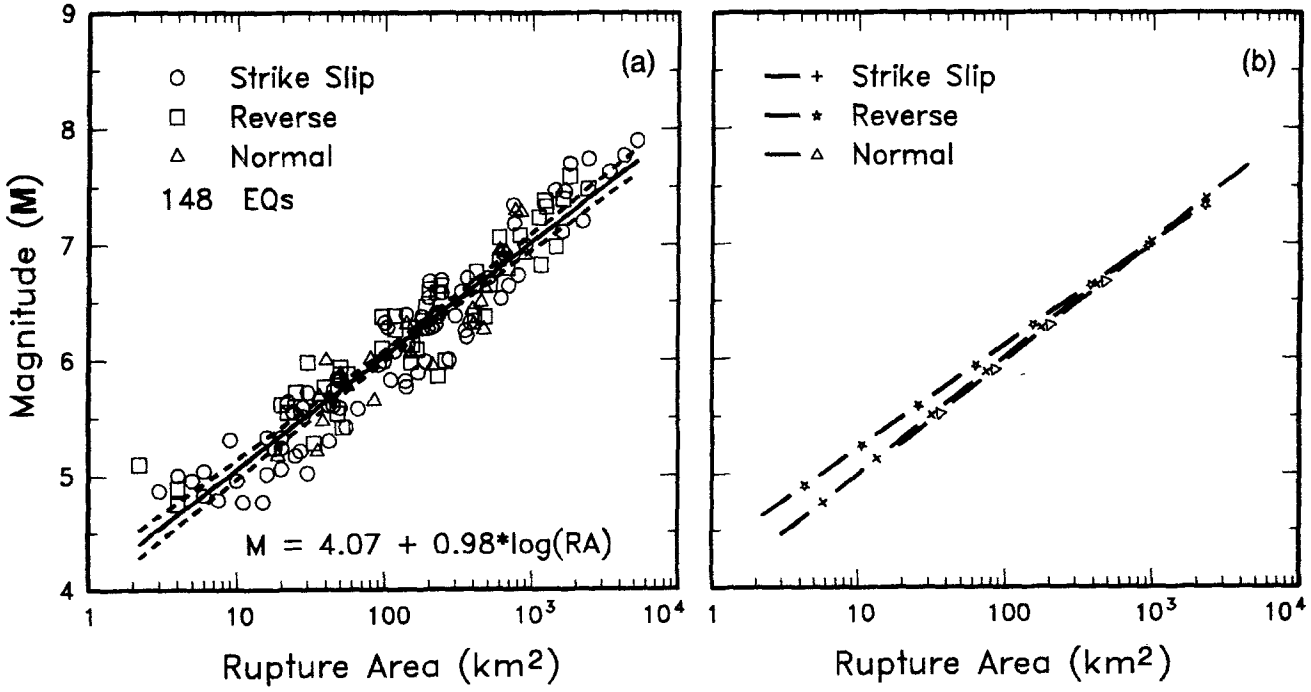

Figure 16. (a) Regression of rupture area on magnitude (M). Regression line shown for all-slip-type relationship. Short dashed line indicates 95% confidence interval. (b) Regression lines for strike-slip, reverse, and normal-slip relationships. See Table 2 for regression coefficients. Length of regression lines shows the range of data for each relationship.

slip regressions indicate an expected magnitude of **M** 6.0, whereas reverse and normal regressions indicate **M** 6.1 and **M** 6.0, respectively. For an expected rupture area of 5000 km^2, all regressions indicate an expected magnitude of **M** 7.7 to 7.8. Differences of more than 0.2 magnitude units occur only at magnitudes less than **M** 5.0. Because the difference in these magnitude estimates is small, the all-slip-type relationship for rupture area versus magnitude is appropriate for most applications. The difference between magnitude estimates for rupture width versus magnitude relationships also is small, thus, the all-slip-type relationship again is preferred for most applications.

In contrast, regressions for displacement relationships show larger differences as a function of slip type. Visually, the positions of regression lines for normal and strike-slip data sets vary somewhat for magnitude versus maximum displacement and magnitude versus average displacement relationships (Figs. 10b and 11b). Applying t statistics to these relationships shows that strike-slip and dip-slip (normal plus reverse) coefficients differ at all significance levels. Normal-slip coefficients do not differ from strike-slip plus reverse coefficients at a 95% significance level. Because strike-slip relationships are well correlated and have low standard deviations ($r \geqq 0.89$ and $s \leqq 0.29$), using these regressions (magnitude versus maximum or average displacement) may be appropriate when the expected slip type is assessed with a high degree of confidence. For situations in which the slip type is uncertain, or for normal and reverse-slip faults, the all-slip-type regression may provide the most reliable results.

Small differences occur in the position of normal and strike-slip regression lines for relationships between displacement and surface rupture length (Figs. 12b and 13b). Evaluation of t statistics for displacement versus surface rupture length relationships shows that normal and strike-slip coefficients do not differ at a 95% significance level. Because the strike-slip regression has the highest correlation (0.86 and 0.82) and the lowest standard deviation (0.36 and 0.32) of the three slip types, for maximum and average displacement regressions, respectively, it may provide the most reliable results when the expected slip type is assessed with a high degree of confidence. The all-slip-type relationship may be appropriate for other situations.

Effects of Data Selection

We evaluated the relative stability of individual relationships with respect to changes in the data set (i.e., addition or deletion of events or changes in the source parameters). We tested the sensitivity of the correlations by removing two data points at random from each data set and recalculating the regression coefficients. Relationships that include more than approximately 14 data points are considered stable because there is no difference at a 95% significance level between the regression coefficients for both data sets. We consider relationships that are based on fewer than 10 data points to be unstable, because changes in these smaller data sets may produce significant changes in the regression coefficients. We also observe that larger data sets typically have higher correlations and lower standard deviations.

It is interesting to note that although there are far more data points for subsurface rupture length and rupture area relationships (for all-slip-type regressions) than for surface rupture relationships, they have only slightly higher correlation coefficients and slightly lower standard deviations (Table 2). This suggests that these three regressions are very stable and are unlikely to change significantly with additional data. Because the surface and subsurface rupture parameters are measured by different techniques, the similar statistical correlation also implies that the variability in the data sets is stochastic in nature, and does not result from errors in measurement techniques. It is expected that variable expression of subsurface ruptures at the surface might result in a weaker correlation between surface rupture length and magnitude than between subsurface rupture length and magnitude. However, both relationships are well correlated and have similar statistical variability.

Effects of Tectonic Setting

Recent studies relate magnitude to rupture length and to displacement and relate seismic moment to rupture length for regions of different geographic setting, tectonic setting, or regional crustal attenuation characteristics (e.g., Acharya, 1979; Wesnousky *et al.*, 1983; Bonilla *et al.*, 1984; Nowroozi, 1985; Khromovskikh, 1989; Slemmons *et al.*, 1989; dePolo *et al.*, 1991; Johnston, 1991). One goal of this study is to evaluate whether the tectonic setting of a region might have a greater effect on regressions than does the type of fault slip. The results of Slemmons *et al.* (1989) suggest that separating data by compressional and extensional settings is insignificant for rupture length relationships, but may be significant for displacement relationships. The data in Table 1 are separated into compressional and extensional settings, and regression coefficients are calculated for each all-slip-type relationship (excluding average displacement). We use t statistics to compare the coefficients (a and b) of extensional and compressional regressions, and we observe no difference between the coefficients at a 95% significance level for any of the relationships. Thus, the difference between the extensional and compressional coefficients is insignificant.

Johnston (1991) calculated regressions of magnitude versus surface rupture length and magnitude versus maximum displacement for data from stable continental regions (SCR's). His results were not significantly different from regressions for non-SCR data sets. We also calculate all-slip-type regressions for the SCR earth-

quakes in our data base and compare these results to data from the rest of the world. Because the SCR data sets for surface rupture length and displacement relationships contain only six to seven earthquakes and the correlations are low ($r < 0.75$), these relationships are not significant at a 95% probability level and are not considered further. Relationships for magnitude versus subsurface rupture length, magnitude versus rupture width, and magnitude versus rupture area comprise 18, 17, and 17 earthquakes, respectively, are well correlated ($r > 0.9$), and are significant at a 95% probability level. Comparing SCR regression coefficients to non-SCR coefficients shows that the rupture area regressions differ at a 95% significance level, whereas the subsurface rupture length and rupture width regression coefficients do not differ at a 95% significance level. We note, however, that the difference in expected magnitudes generally is small (less than 0.2 M) for these regressions (Fig. 17). These results indicate that subdividing our data set according to various tectonic settings or geographic regions does not greatly improve the statistical significance of the regressions.

Discussion

The primary purpose of developing regression relationships among various earthquake source parameters is to predict an expected value for a dependent parameter from an observed independent parameter. Because we calculate the regressions by the method of ordinary least squares, the coefficients presented in Table 2 are for estimating the dependent variable. The independent and dependent variables will depend on the application—either the expected magnitude for a given fault parameter, or the expected fault parameter for a given magnitude. Table 2 gives the normal and inverted regression coefficients as a function of the sense of slip.

Note that the values of dependent variables derived from these regression formulas are *expected* values. Thus, the calculated values are expected to be exceeded in 50% of the earthquakes associated with the given value of the independent variable. Bonilla *et al.* (1984) discuss techniques for evaluating dependent variables at lower exceedance probabilities. In addition, the formulas in Table 2 are not applicable to values of the independent variable that lie outside the data range listed for each regression.

The empirical relationships presented here can be used to assess maximum earthquake magnitudes for a particular fault zone or an earthquake source. The assumption that a given magnitude is a *maximum* value is valid only if the input parameter, for instance the rupture length, also is considered a maximum value. For example, suppose we are interested in assessing the maximum magnitude that a fault is capable of generating, and that we have sufficient data to estimate the possible length and downdip width of future ruptures. Evaluating the segmentation of a fault zone (e.g., Schwartz and Copper-

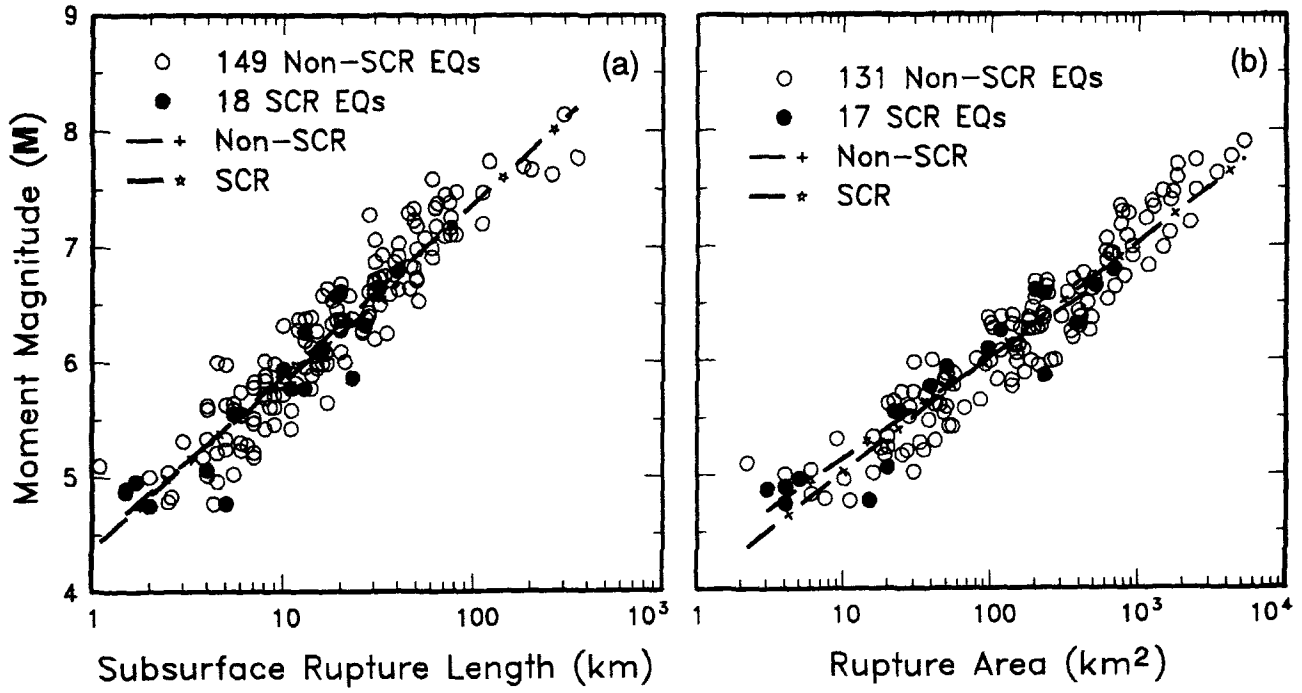

Figure 17. Regression lines for stable continental region (SCR) earthquakes and non-SCR continental earthquakes. (a) Regression of surface rupture length on magnitude (M). (b) Regression of rupture area on magnitude (M).

smith, 1986) provides a basis for assessing the maximum length of future ruptures. The depths of earthquake hypocenters, together with the dip of the fault, limit the maximum downdip width of future ruptures. Given that the length and width are assessed to be maximum values, empirical relations between magnitude and rupture length and rupture area will provide the expected maximum magnitudes. These are *expected* maximum magnitudes for the given maximum fault parameters. However, because there is dispersion associated with the statistical relations, both higher and lower magnitudes are possible for any single event having the given rupture parameters. The standard deviation for each regression provides a measure of that dispersion.

Regarding regressions between magnitude and subsurface rupture length and rupture area, previous studies indicate that the size and depth of the earthquake, as well as the nature of near-surface materials, have a significant effect on whether the subsurface rupture is partly or fully expressed by faulting at the surface (e.g., Amaike, 1987; Berberian and Papastamatiou, 1978; Bernard and Zollo, 1989; Bonilla, 1988). In addition, the absence of surface rupture during some large-magnitude earthquakes (greater than **M** 7), and the occurrence of surface rupture for some smaller-magnitude earthquakes (less than **M** 5.5), show that there are large variations in rupture at the surface. Thus, variation in the geologic conditions and the hypocentral depths of future earthquakes will have uncertain effects on the extent of future surface ruptures. In contrast, subsurface rupture length and rupture area, which are estimated from the spacial distribution of aftershocks, are not subject to these uncertainties. For example, in the subsurface, earthquakes typically appear to rupture individual fault segments, and the segment boundaries are defined at the surface by various geometric, structural, or geologic features (Knuepfer, 1989). During some earthquakes, however, even though an entire segment ruptures in the subsurface, the rupture may not propagate over the full length of the segment at the ground surface. Thus, we believe that subsurface rupture length regressions are appropriate for estimating magnitudes for expected ruptures along single or multiple fault segments. Where the extent of previous ruptures at the surface can be evaluated, however, surface rupture length regressions are appropriate for estimating expected magnitudes. Applying subsurface rupture length and rupture area relations to estimating magnitudes may help to overcome uncertainties associated with estimating the surface rupture length for some seismic sources.

The regressions for subsurface rupture length and rupture area also provide a basis for estimating the magnitudes of earthquakes that may occur on subsurface seismic sources such as blind thrust faults, which cannot be evaluated from surface observations. Furthermore, regressions on subsurface parameters include data for moderate-magnitude earthquakes (in the range of magnitude 5 to 6), allowing the characterization of relatively small seismic sources that may not rupture the surface.

The use of empirical regressions to assess maximum magnitudes typically involves developing several magnitude estimates from which a maximum magnitude value is selected or an uncertainty distribution is constructed. Various segmentation models have been proposed to define the reaches of a fault zone that are relatively continuous and behave similarly (Schwartz and Coppersmith, 1986; Schwartz, 1988). Estimates of the possible lengths of future ruptures involve considering the possibilities that one or more of these segments might rupture. Alternative rupture scenarios and associated rupture lengths result in multiple estimates of earthquake magnitude using a single regression relationship, such as surface rupture length versus magnitude or subsurface rupture length versus magnitude. Further, if the downdip geometry of a fault zone is known, the rupture width and rupture area relationships provide additional magnitude estimates. Detailed geologic studies along a fault zone can result in estimates of the maximum and average displacement associated with individual paleoseismic events along the fault zone. These displacement estimates also may be used with the appropriate regressions to assess expected magnitudes. Ultimately, developing a maximum magnitude estimate involves judging which rupture scenarios are most credible, which rupture parameters (e.g., rupture length, area, and displacement) represent *maximum* parameters, and the relative preference for the various regressions (perhaps based on the dispersion associated with each regression). For probabilistic seismic hazard analyses, these considerations and estimates may be combined into a probabilistic distribution of the maximum magnitude (Coppersmith, 1991).

In addition to assessing maximum magnitudes, the regressions presented in this study have other potential engineering applications. For example, seismic design criteria for facilities such as pipelines and tunnels require estimates of the amount of displacement that might occur where the facility crosses a fault. The regressions of displacement on magnitude provide the expected values for a given earthquake magnitude. In particular, the *average* displacement regression provides the mean displacement along the length of a rupture, and the *maximum* displacement regression provides the expected largest slip at a point along a rupture. In most applications, the average displacement is desired because it is unknown, prior to a rupture event, whether the facility lies at the point where the maximum displacement will occur. The maximum displacement regression might be used to provide a conservative upper bound for engineering design.

Conclusions

The data base reveals that surface rupture length typically is equal to 75% of the subsurface rupture length,

and the average surface displacement typically is equal to one-half of the maximum surface displacement. The ratio of surface rupture length to subsurface rupture length increases slightly as magnitude (**M**) increases. There is no apparent relationship between the ratio of average displacement to maximum displacement and magnitude (**M**). We calculate the average subsurface displacement on the fault plane from the rupture area and the seismic moment; this is more than the average displacement and less than the maximum displacement measured at the surface. Thus, for many earthquakes in our data base, most slip on the fault plane at seismogenic depths propagates to the surface. We also note that there is no systematic difference between M_S and **M** for the events in the data base over the range of magnitude 5.7 to 8.0. However, M_S is systematically smaller than **M** for magnitudes less than 5.7.

The empirical regressions show a strong correlation between magnitude and various rupture parameters, which enables us confidently to use these relationships to estimate magnitudes or rupture parameters. The regressions between magnitude and surface rupture length, subsurface rupture length, downdip rupture width, and rupture area are well determined in most cases, having correlation coefficients of about 0.84 to 0.95 and standard deviations of about 0.24 to 0.41 magnitude units. Relationships between displacement and rupture length or magnitude are less well correlated (correlation coefficient about 0.71 to 0.78).

In most cases, the empirical regressions do not vary significantly as a function of the sense of slip. The t statistics show that the regression coefficients are not different at high significance levels for regressions between magnitude and surface rupture length, and magnitude and subsurface rupture length. Relationships between magnitude and rupture area, and magnitude and rupture width, are different at a 95% significance level. The regression coefficients are similar, however, and differences in parameters estimated from these regressions typically are small. This conclusion suggests that the all-slip-type regression may be used for most situations, and is especially significant for evaluating expected magnitudes for poorly known faults or blind faults that lack clear surface expression. The regressions of displacement versus magnitude show a mild dependency on the sense of slip in some cases; however, these relationships have the weakest statistical correlations.

Analysis of data sets of various sizes shows that regressions containing approximately 14 or more data points are insensitive to changes in the data. Smaller data sets (less than 10 to 14 data points) generally are sensitive to changes in the data, and correlations may not be significant. The regressions for subsurface rupture length and rupture area are based on the largest data sets, yet show statistical correlations similar to those of the smaller data set for surface rupture length regressions. This suggests that the relationships based on large data sets (more than 50 earthquakes) are unlikely to change significantly with the addition of new data.

In evaluating dependency of the relationships on tectonic setting we compare the coefficients (a and b) of extensional and compressional regressions for each relationship using t statistics. We observed no difference between the coefficients at a 95% significance level for any of the relationships; thus, the difference between the extensional and compressional coefficients is small. We calculate all-slip-type regressions for the SCR earthquakes in our data base and compare these results to data from the rest of the world. Comparing SCR regression coefficients to non-SCR coefficients shows that the rupture area regressions differ at a 95% significance level, whereas the subsurface rupture length regressions do not differ at this significance level. These results indicate that subdividing the data set according to various tectonic settings or geographic regions occasionally may provide slightly different results, but typically does not improve the statistical significance of the regressions.

Because of the larger number of data and good statistical correlations, we believe that the all-slip-type regressions are appropriate for most applications of these regressions. The use of the regressions for subsurface rupture length and rupture area may be appropriate where it is difficult to estimate the near-surface behavior of faults, such as for buried or blind faults. Reliable estimates of the maximum expected magnitude for faults should include consideration of multiple estimates of the expected magnitude derived from various rupture parameters.

Acknowledgments

We thank Pacific Gas & Electric Company (San Francisco) for financial support of this study. Dr. Robert Youngs (Geomatrix Consultants) provided extensive assistance in the statistical analysis of the data sets. Dr. David Burton Slemmons and Mr. Zhang Xiaoyi (University of Nevada, Reno) contributed the preliminary results of their studies of average surface displacements for historical earthquakes. We are grateful for the expertise Dr. Slemmons provided in evaluating the surface rupture lengths and displacements for many of the earthquakes in the data base. We also wish to thank Dr. William Savage and Dr. Janet Cluff (Pacific Gas & Electric Company), Dr. Slemmons, and an anonymous reviewer for careful evaluations of drafts of this article.

References

Abe, K. (1981). Magnitudes of large shallow earthquakes from 1904–1980, *Phys. Earth Planet. Interiors* **27**, 72–92.

Abe, K. and S. Noguchi (1983a). Determination of magnitude for large shallow earthquakes 1898–1917, *Phys. Earth Planet. Interiors* **32**, 45–59.

Abe, K. and S. Noguchi (1983b). Revision of magnitudes of large shallow earthquakes, 1897–1912, *Phys. Earth Planet. Interiors* **33**, 1–11.

Acharya, H. K. (1979). Regional variations in the rupture-length

magnitude relationships and their dynamical significance, *Bull. Seism. Soc. Am.* **69**, 2063–2084.

Aki, K. and P. G. Richards (1980). *Quantitative Seismology, Volume I*, W. H. Freeman, San Francisco, 512 pp.

Albee, A. L. and J. L. Smith (1966). Earthquake characteristics and fault activity in southern California, in *Engineering Geology in Southern California*, R. Lung and D. W. Proctor (Editors), Association of Engineering Geologists, Los Angeles Section, 9–34.

Amaike, F. (1987). Seismic explorations of the buried fault associated with the 1948 Fukui earthquake, *J. Phys. Earth* **35**, 285–308.

Ambraseys, N. N. (1975). Studies in historical seismicity and tectonics, in *Geodynamics Today*, The Royal Society, London, 7–16.

Ambraseys, N. N. (1988). Engineering seismology, *Earthquake Eng. Struct. Dyn.* **17**, 1–105.

Benjamin, J. R. and C. A. Cornell (1970). *Probability, Statistics, and Decision for Civil Engineers*, McGraw-Hill, New York, 684 pp.

Berberian, M. and D. Papastamatiou (1978). Khurgu (north Bandar Abbas, Iran) earthquake of 21 March 1977—a preliminary field report and a seismotectonic discussion, *Bull. Seism. Soc. Am.* **68**, 411–428.

Bernard, P. and A. Zollo (1989). The Irpinia (Italy) 1980 earthquake—detailed analysis of a complex normal faulting, *J. Geophys. Res.* **94**, 1631–1647.

Bonilla, M. G. (1988). Minimum earthquake magnitude associated with coseismic surface faulting, *Bull. Assoc. Eng. Geologists* **25**, 17–29.

Bonilla, M. G. and J. M. Buchanon (1970). Interim report on worldwide historic surface faulting, *U.S. Geol. Surv. Open-File Rept. 70-34*, 32 pp.

Bonilla, M. G., R. K. Mark, and J. J. Lienkaemper (1984). Statistical relations among earthquake magnitude, surface rupture length, and surface fault displacement, *Bull. Seism. Soc. Am.* **74**, 2379–2411.

Boore, D. M. and W. B. Joyner (1982). The empirical prediction of ground motion, *Bull. Seism. Soc. Am.* **72**, S43–S60.

Chinnery, M. A. (1969). Earthquake magnitude and source parameters, *Bull. Seism. Soc. Am.* **59**, 1969–1982.

Clark, M. M. (1972). Surface rupture along the Coyote Creek fault, in *The Borrego Mountain Earthquake of April 9, 1968, U.S. Geol. Surv. Profess. Pap. 787*, 55–86.

Coppersmith, K. J. (1991). Seismic source characterization for engineering seismic hazard analysis, in *Proc. 4th International Conference on Seismic Zonation*, Vol. I, Earthquake Engineering Research Institute, Oakland, California, 3–60.

Darragh, R. B. and B. A. Bolt (1987). A comment on the statistical regression relation between earthquake magnitude and fault rupture length, *Bull. Seism. Soc. Am.* **77**, 1479–1484.

Davis, J. C. (1986). *Statistics and Data Analysis in Geology*, Second Ed., Wiley, New York, 646 pp.

dePolo, C. M., D. G. Clark, D. B. Slemmons, and A. R. Ramelli (1991). Historical surface faulting in the Basin and Range province, western North America: implications for fault segmentation, *J. Struct. Geol.* **13**, 123–136.

Dietz, L. D. and W. L. Ellsworth (1990). The October 17, 1989, Loma Prieta, California, earthquake and its aftershocks: geometry of the sequence from high-resolution locations, *Geophys. Res. Lett.* **17**, 1417–1420.

Duda, S. J. (1965). Secular seismic energy release in the circum-Pacific belt, *Tectonophysics* **2**, 409–452.

Dziewonski, A. M., T.-A. Chow, and J. H. Woodhouse (1981). Determination of earthquake source parameters from waveform data for studies of global and regional seismicity, *J. Geophys. Res.* **86**, 2825–2852.

Electric Power Research Institute (1987). Seismic hazard methodology for the central and eastern United States—Volume 1: *Methodology, Report NP-4726*, prepared for Seismicity Owners Group and Electric Power Research Institute under research projects P101-38, -45, -46, 2256–14.

Gubbins, D. (1990). *Seismology and Plate Tectonics*, Cambridge University Press, Cambridge, England, 339 pp.

Gutenberg, B. (1945). Amplitudes of surface waves and magnitudes of shallow earthquakes, *Bull. Seism. Soc. Am.* **34**, 2–12.

Gutenberg, B. and C. F. Richter (1954). *Seismicity of the Earth and Associated Phenomena*, Second Ed., Princeton University Press, Princeton, New Jersey, 310 pp.

Hanks, T. C. and H. Kanamori (1979). A moment-magnitude scale, *J. Geophys. Res.* **84**, 2348–2350.

Hanks, T. C. and M. Wyss (1972). The use of body-wave spectra in the determination of seismic-source parameters, *Bull. Seism. Soc. Am.* **62**, 561–589.

Hanks, T. C., J. A. Hileman, and W. Thatcher (1975). Seismic moments of the larger earthquakes of the southern California region, *Geol. Soc. Am. Bull.* **86**, 1131–1139.

Iida, K. (1959). Earthquake energy and earthquake fault, Nagoya University, *J. Earth Sci.* **7**, 98–107.

Johnston, A. C. (1991). Surface rupture in stable continental regions, *EOS* **72**, 489.

Johnston, A. C. and L. R. Kanter (1990). Earthquakes in stable continental crust, *Scientific American* **262**, 68–75.

Kanamori, H. (1983). Magnitude scale and quantification of earthquakes, *Tectonophysics* **93**, 185–199.

Kanamori, H. and D. L. Anderson (1975). Theoretical basis of some empirical relations in seismology, *Bull. Seism. Soc. Am.* **65**, 1073–1096.

Khromovskikh, V. S. (1989). Determination of magnitudes of ancient earthquakes from dimensions of observed seismodislocations. *Tectonophysics* **166**, 269–280.

Knuepfer, P. L. K. (1989). Implications of the characteristics of endpoints of historical surface fault ruptures for the nature of fault segmentation, in *Proc. of Conf. XLV, Fault Segmentation and Controls of Rupture Initiation and Termination*, D. P. Schwartz and R. H. Sibson (Editors), *U.S. Geol. Surv. Open-File Rept. 89-315*, 193–228.

Lee, W. H. K., F. T. Wu, and S. C. Wang (1978). A catalog of instrumentally determined earthquakes in China (magnitude > 6) compiled from various sources, *Bull. Seism. Soc. Am.* **68**, 383–398.

Lienkaemper, J. J. (1984). Comparison of two surface-wave magnitude scales—M of Gutenberg and Richter (1954) and M_S of "preliminary determination of epicenters," *Bull. Seism. Soc. Am.* **74**, 2357–2378.

Mendoza, C. and S. H. Hartzell (1988). Aftershock patterns and main shock faulting, *Bull. Seism. Soc. Am.* **78**, 1438–1449.

Nowroozi, A. A. (1985). Empirical relations between magnitudes and fault parameters for earthquakes in Iran, *Bull. Seism. Soc. Am.* **75**, 1327–1338.

Ohnaka, M. (1978). Earthquake-source parameters related to magnitude, *Geophys. J. R. Astr. Soc.* **55**, 45–66.

Panza, G. F., S. J. Duda, L. Cernobori, and M. Herak (1989). Gutenberg's surface-wave magnitude calibrating function: theoretical basis from synthetic seismograms, *Tectonophysics* **166**, 35–43.

Purcaru, G. and H. Berckhemer (1982). Quantitative relations of seismic source parameters and a classification of earthquakes, in *Quantification of Earthquakes*, S. J. Duda and K. Aki (Editors), *Tectonophysics* **84**, 57–128.

Richter, C. F. (1958). *Elementary Seismology*, W. H. Freeman, San Francisco, 768 pp.

Rothe, J. P. (1969). *The Seismicity of the Earth, 1953–1965*. UNESCO, Paris.

Scholz, C. H. (1982). Scaling laws for large earthquakes: consequences for physical models, *Bull. Seism. Soc. Am.* **72**, 1–14.

Schwartz, D. P. (1988). Geology and seismic hazards: moving into the 1990's, in *Earthquake Engineering Soil Dynamics II—Recent Advances in Ground Motion Evaluation*. Vol. 20, J. L. Van Thun (Editor), American Society of Civil Engineers Geotechnical Special Publication, New York, 1–42.

Schwartz, D. P. and K. J. Coppersmith (1986). Seismic hazards—new trends in analysis using geologic data, in *Active Tectonics*, National Academy Press, Washington, D.C., 215–230.

Sibson, R. H. (1987). Effects of fault heterogeneity on rupture propagation, in *Proc. of Conf. XXXIX, Directions in Paleoseismology*, A. J. Crone and E. M. Omdahl (Editors), *U.S. Geol. Surv. Open-File Rept. 87-673*, 362–373.

Singh, S. K., E. Bazan, and L. Esteva (1980). Expected earthquake magnitude from a fault, *Bull. Seism. Soc. Am.* **70**, 903–914.

Slemmons, D. B. (1977). Faults and earthquake magnitude, U.S. Army Corps of Engineers, Waterways Experimental Station, Miscellaneous Papers S-73-1, Report 6, 1–129.

Slemmons, D. B. (1982). Determination of design earthquake magnitudes for microzonation, *Proc. of the Third International Earthquake Microzonation Conf.* Vol. 1, U.S. National Science Foundation, Washington, D.C., 119–130.

Slemmons, D. B., P. Bodin, and X. Zang (1989). Determination of earthquake size from surface faulting events, *Proc. of the International Seminar on Seismic Zonation*, Guangzhou, China, State Seismological Bureau, Beijing, 13.

Tocher, D. (1958). Earthquake energy and ground breakage, *Bull. Seism. Soc. Am.* **48**, 147–153.

Troutman, B. M. and G. P. Williams (1987). Fitting straight lines in the earth sciences, in *Use and Abuse of Statistical Methods in the Earth Sciences*, W. B. Size (Editor), Oxford University Press, New York, 107–128.

Utsu, T. (1969). Aftershocks and earthquake statistics (I), some parameters which characterize an aftershock sequence and their interrelations, *J. Faculty Sci.*, Series VII, Vol. III, Hokkaido University, Japan, 129–195.

Utsu, T. and A. Seki (1954). A relation between the area of aftershock region and the energy of main-shock, *J. Seism. Soc. Japan* **7**, 233–240.

Wesnousky, S. G. (1986). Earthquakes, Quaternary faults, and seismic hazards in California, *J. Geophys. Res.* **91**, 12587–12631.

Wesnousky, S. G., C. H. Scholz, K. Shimazaki, and T. Matsuda (1983). Earthquake frequency distribution and mechanics of faulting, *J. Geophys. Res.* **88**, 9331–9340.

Wu, F. T. (1968). Parkfield earthquake of 28 June 1966—magnitude and source mechanism, *Bull. Seism. Soc. Am.* **58**, 689–709.

Wyss, M. (1979). Estimating maximum expectable magnitude of earthquakes from fault dimensions, *Geology* **7**, 336–340.

Geomatrix Consultants, Inc.
San Francisco, California 94111

Manuscript received 22 March 1993.